Poly (vinyl alcohol)/Pullulan/NaCl Conductive Hydrogels for Wearable Strain Sensors

Xiaoyan Qing [a], Zhongda Liu [b], Alexandros Katsaounis [b], Nikolaos Bouropoulos [c,d], Irene Taurino [e,f], Pedro Fardim [a,*]

[a] Chemical and Biochemical Reactor Engineering and Safety (CREaS), Department of Chemical Engineering, KU Leuven, Celestijnenlaan 200f, 3001 Leuven, Belgium. xiaoyan.qing@kuleuven.be

[b] Department of Chemical Engineering, University of Patras, Caratheodory 1 St, 26504 Patras, Greece. zhongda.liu@chemeng.upatras.gr; alex.katsaounis@chemeng.upatras.gr

[c] Department of Materials Science, University of Patras, 26504 Patras, Greece

[d] Foundation for Research and Technology Hellas, Institute of Chemical Engineering and High Temperature Chemical Processes, Stadiou Street, Platani, 26504 Patras, Greece. nbouro@upatras.gr

[e] Micro and Nano Systems (MNS), Department of Electrical Engineering, KU Leuven, 3001 Leuven, Belgium

[f] Semiconductor Physics, Department of Physics and Astronomy, KU Leuven, Celestijnenlaan 200d, 3001 Leuven, Belgium. irene.taurino@kuleuven.be

*Email: pedro.fardim@kuleuven.be

Abstract

Ionic conductive hydrogels have emerged as promising candidates for wearable sensors thanks to their stretchability and conductivity. However, it is still challenging to fabricate hydrogels simultaneously with balanced mechanical strength, ionic conductivity, and sensitivity. In this work, PVA/Pullulan/NaCl ionic hydrogels were prepared by soaking frozen-thawed PVA/Pullulan hydrogels in NaCl solutions. Due to the synergy of the semi-interpenetrating network between PVA and pullulan as well as the salting-out effect due to NaCl, the hydrogels exhibited a large tensile strength of 2.72 MPa. The presence of Na^+ and Cl^- ions endowed the hydrogels with superb ionic conductivity (up to 10.44 S/m). The hydrogel was assembled as a strain sensor, which displayed good sensitivity (up to 5.98) and was utilized for the detection of human joint movements. Additionally, hydrogel sensors can provide efficient information transmission through Morse code. As such, the presented PVA/Pullulan/NaCl hydrogels suggested a promising prospect for the next generation of wearable sensors.

Keywords: PVA ionic conductive hydrogel; strain sensor

1. Introduction

The growth of the Internet of Things has boosted the dramatic development of wearable electronics in recent years [1]. Conductive hydrogels have received considerable attention in human motion detection, health monitoring, electronic skins, and flexible supercapacitors [2-6] because they possess both the conductivity of conductive components and the stretchability of hydrogels. The conductivity mechanism can be divided into electronic and ionic conduction. Electronic conductivity is normally achieved by adding conductive fillers and conductive polymers into the hydrogel matrix. By doing so, the hydrogels show high conductivity, but the conductive components lack hydrophilicity and poorly disperse in the hydrogels. In contrast, ions are more compatible with the hydrogel and ionic conductive hydrogels have gained much interest due to their facile processibility [7].

Currently, ionic conductive hydrogels have been studied in wearable sensors and researchers have extensively optimised the mechanical properties and enhanced ionic conductivity. Polyvinyl alcohol (PVA) as a typical synthetic polymer has been widely used as the hydrogel matrix for ionic conductive hydrogels because of its commercial availability, hydrophilicity, and non-toxicity. By introducing ions into PVA hydrogel matrix, the ionic conductivity can be as high as 8.16–12.5 S/m [8, 9]. Regardless of the impressive ionic conductivity, there exists a trade-off between high ionic conductivity and mechanical strength, such as PVA/sodium alginate/collagen/NaCl hydrogels had a high conductivity of 3.8 S/m but a low tensile strength 390 kPa [10].

High mechanical strength is needed for conductive hydrogels in wearable sensors since it can avoid premature failure during various mechanical loads. Consequently, some strategies are commonly used to improve the mechanical properties: 1) constructing a double network [11]; 2) doping nanocomposites into the hydrogels [12, 13]. However, toxic crosslinkers are inevitably used for the construction of double networks and the commonly used monomers, like acrylamide, and acrylic acid, have been classified as hazardous substances by ECHA [14], which is user-unfriendly. On the other hand, nanocomposites can pose harmful effects on humans, plants, animals, and the

environment, which deviate from the idea of environmental sustainability. As a promising sustainable alternative, the exploration of biobased biopolymers in recent years has been fast-growing. Biobased biopolymers feature biodegradability, environmental friendliness, manipulated mechanical properties and biocompatibility [15]. Until now, some mainstream biopolymers such as cellulose, chitosan, and sodium alginate have been extensively investigated as mechanical reinforcers and display versatile wearable applications [16-19]. In addition to these biopolymers, pullulan is rapidly emerging as an important source of biobased biopolymers, but the potential in wearable sensors has not been much explored. Pullulan is an exopolysaccharide obtained from the fermentation of *Aureobasidium pullulans*. Pullulan shows high water solubility even in cold water, biocompatibility, and non-toxicity and has been approved as a safe compound by the FDA and European Union [20]. The blends of pullulan and PVA can show high mechanical properties, but the PVA/Pullulan composites were in the form of dried film [21]. Recently, composite hydrogels made from PVA/Pullulan were used as a platform for drug delivery, tissue engineering and wound dressing, but neither the mechanical properties nor the potential in wearable sensors has been explored [22-24]. Good mechanical properties are prerequisites to extend the scenarios. Thus, it is necessary to study the relevant mechanical properties of PVA/Pullulan hydrogels and broaden the application in wearable sensors. Furthermore, kosmotropic salts like SO_4^{2-}, CO_3^{2-}, and Cl^- can weaken the hydration of the hydrophilic polymer chains and induce dense structure, thereby the salting-out effect has also been adopted to improve mechanical strength as well. Nonetheless, low ionic conductivity is observed during the long soaking process [25-30]. Thus, the soaking time needs to be considered with the aim of balanced mechanical properties and ionic conductivity.

For a specific application, e.g. wearable strain sensor, sensitivity (represented by gauge factor (GF)) is an unignorable aspect. Nevertheless, the simultaneous achievement of high sensitivity with balanced mechanical strength and conductivity is still challenging for PVA ionic conductive hydrogels. Physically crosslinked hydroxypropyl cellulose/PVA/NaCl hydrogels exhibited both a high tensile strength of 1.3 MPa and conductivity of 3.4 S/m, but the GF (0.947) was relatively low [31]. The cellulose nanofibrils and $ZnSO_4$ reinforced PVA conductive hydrogels had a large tensile strength of 0.79 MPa and an improved GF of 1.7 but with a low conductivity of 0.32 S/m [32]. PVA/ethanol/$FeCl_3$ organo-hydrogels simultaneously obtained a high mechanical strength of 6.5 MPa, high conductivity of 6.5 S/m and high GF of 3.1. However, $FeCl_3$ is highly corrosive and irritant [33]. Thus, balanced ionic conductivity, mechanical strength, and high sensitivity as well as the safety and sustainability of the materials should be considered for wearable sensors.

In this work, we prepared PVA/Pullulan/NaCl conductive hydrogels with balanced mechanical strength, ionic conductivity and high sensitivity through the freezing-thawing method followed by the NaCl soaking process. All the raw materials in this work are nontoxic and biodegradable, which accords with the concept of sustainability. We take the leverage of biopolymer and salting-out effect to synergistically improve the mechanical properties. The hydrogen bonds and entanglement between pullulan and PVA (semi-interpenetrate network), as well as the NaCl-induced polymer aggregation (salting-out effect) had a synergistic effect for tunable mechanical strength (0.48–2.72 MPa). NaCl is easily available at low cost and safer than other commonly used inorganic

metal salts (LiCl, $ZnCl_2$, $FeCl_3$, etc.). A long-time soaking can induce high mechanical strength, but it also comes with a low ionic conductivity or GF [34, 35], and thus we proposed 2 h soaking to balance these properties. Benefiting from this, the ionic conductivity ranged from 2.43–10.44 S/m and GF maximumly reached 5.98. In general, we demonstrated that PVA/Pullulan/NaCl ionic conductive hydrogels had potential applications in wearable sensors, such as human motion monitoring and information communication. We believe this hydrogel strain sensor brings us closer towards sustainable wearable electronics.

2. Materials and Methods

2.1 Materials

Polyvinyl alcohol (PVA) (molecular weight (MW) = 72 kDa, degree of hydrolysis >98%) was obtained from Merck Schuchardt OHG. Pullulan was purchased from TCI and the MW was determined as shown in **Figure S1**. Sodium chloride (NaCl) was purchased from Sigma-Aldrich. $NaNO_3$ (assay 99%–100.5%) was purchased from Honeywell.

2.2 Preparation of stock solutions

PVA powder was dissolved in deionized (DI) water with magnetic stirring in 90 °C water bath for 3 h. After cooling down, 12 wt% of PVA solution was obtained. The 12 wt% of pullulan solution was prepared by dissolving pullulan powder in DI water at room temperature. Different concentrations of NaCl solutions (0.3–5 M) were obtained by dissolving NaCl in DI water.

2.3 Fabrication of PVA/Pullulan/NaCl hydrogels

The PVA/Pullulan/NaCl hydrogels were synthesized by the freezing-thawing method followed by a soaking process. First, 12 wt% of PVA solution and 12 wt% pullulan solution were mixed with the desired mass ratio at room temperature. Then, the mixture was transferred into PTFE molds and subjected to freezing at −20 °C for 3 h and thawing at room temperature for 1 h. The freezing-thawing process was implemented for three cycles to obtain the PVA/pullulan hydrogels. Subsequently, the PVA/Pullulan hydrogels were immersed in NaCl solutions (0–5 M) for 2 h and then rinsed with DI water. The resultant hydrogels were denoted as PVA_x/$Pullulan_y$/$NaCl_z$, where x and y represent the mass content (wt%) of PVA and pullulan in the total polymer, respectively and z denotes NaCl concentration (M). For comparison, pure PVA hydrogels (12 wt% total polymer content) were also soaked in NaCl solution (0–5 M). The specific compositions are shown in **Table S1**.

2.4 Characterization

2.4.1 Attenuated total reflection-Fourier transform infrared spectroscopy (ATR-FTIR)

The functional groups of the raw materials (PVA, pullulan) and hydrogels were identified using Fourier transform infrared spectroscopy (IRTracer-100, Shimadzu Corporation, Kyoto, Japan) at the transmittance mode. The hydrogels were freeze-dried and cut into small pieces. The spectra were recorded in the wavenumber range of 4000–500 cm^{-1} with an average of 25 scans at a resolution of 4 cm^{-1}.

2.4.2 Scanning electron microscopy-energy dispersive X-ray analysis (SEM-EDX)

The fresh hydrogels were quickly frozen in liquid nitrogen and then freeze-dried. The samples were coated with a thin film of gold/palladium. Then, the cross-sectional morphology of the dried hydrogels was observed on a scanning electron microscope (SEM, JSM-6010 LV, JEOL Lit. Tokyo, Japan) at an acceleration voltage of 12 kV. The element distribution was analyzed on a scanning electron microscope (Zeiss EVO MA10, Zeiss, Jena, Germany) equipped with energy-dispersive X-ray spectroscopy (EDX) (INCAx-act attachment, Oxford Instruments, Abingdon, UK).

2.4.3 X-ray diffraction (XRD)

The crystal structures of the raw materials and hydrogels were characterized by X'Pert PRO diffractometer (PANalytical, Almelo, The Netherlands) with a Cu tube (Kα λ = 1.5418 Å) and a generator set at 45 kV and 40 mA. A continuous scan mode was applied with the scanning degree range from 4 to 40° and a step size of 0.0167°. The data were analyzed on the software X'Pert Data Viewer (Version 1.9a, PANalytical B.V., Almelo, The Netherlands).

2.4.4 Differential scanning calorimeter (DSC)

The hydrogel samples were sealed in hermetically aluminium pan for DSC measurement (DSC Q2000, TA instrument). The samples (8–9 mg) were cooled from 20 to −70 °C at a rate of 10 °C/min and equilibrated at −70 °C for 5 min, then back to 20 °C. The nitrogen gas at a flow rate of 50 mL/min.

2.4.5 Gel permeation chromatography (GPC)

The molecular weight of pullulan was determined by gel permeation chromatography (GPC) on Malvern's OMNISEC system (Malvern Panalytical, Malvern, UK) equipped with Column A 6000 M (< 20.000000 g/mol). Pullulan was dissolved in DI water with a concentration of 2 mg/mL. The pullulan samples were filtered through a 0.2 µm PES syringe filter and the injection volume was 100 µL. The mobile phase was $NaNO_3$ (0.1 M) with a flow rate of 0.8 mL/min. The results were analyzed on the software OMNISEC v 11.32 (Malvern Panalytical Ltd., Malvern, UK).

2.5 Size change and water content determination

The size change of PVA/Pullulan hydrogels after soaking in NaCl (0–5 M) solution was determined by **Equation 1**. The size of the samples was the same as the samples of the mechanical test.

$$Size\ change\ rate\ (\%) = \frac{L - L_0}{L_0} \times 100 \quad (1)$$

where L_0 and L are the dimensions (mm) before and after soaking.

The water content of PVA/Pullulan/NaCl hydrogels was calculated by measuring the mass before and after drying using **Equation 2** [31]. The size of the samples before soaking was 10 mm × 10 mm × 2 mm.

$$Water\ content\ (\%) = \frac{m_w - m_d}{m_w} \times 100 \quad (2)$$

where m_w and m_d denote the mass (g) of the wet and dried hydrogels, respectively.

2.6 Mechanical properties

The mechanical performance of the hydrogels was evaluated on a universal testing machine with a capacity of 2 kN (Instron 2519-106, USA) at ambient conditions. For the uniaxial tensile tests, the hydrogels were molded into dumbbell shape with the dimension of Type I following the international standard ISO-37-2017(E). The hydrogel specimens were stretched at a constant rate of 50 mm/min until fracture. The test was repeated with 10 parallel samples. The toughness of the hydrogels was determined by integrating the area of the stress-strain curve. Young's modulus was calculated from the slope of the stress-strain curve in the linear region with strain changes from 0% to 20%.

Regarding the cyclic loading-unloading tests, the hydrogel specimens were shaped into rectangle (80 mm × 10 mm × 2 mm). The samples were stretched to different maximum strains (40%, 60%, 80%) and then returned to the initial state at a speed of 200 mm/min. The area between the loading-unloading curve represents the energy dissipation. Each sample was repeated in triplicate.

2.7 Electrical measurements

2.7.1 Conductive property

The electrochemical impedance spectroscopy (EIS) was performed on Autolab (PGSTAT204, Metrohm Autolab B.V., The Netherlands). The measurements were implemented under the open circuit potential with the frequency from 10^{-1} to 10^{5} Hz and an AC amplitude of 10 mV at room temperature. The hydrogel samples (thickness: 2–3.5 mm, length: 9–13 mm, width: 9–12 mm) were sandwiched between two copper electrodes. The ionic conductivity (σ, S/m) of the hydrogels was calculated with **Equation 3**:

$$\sigma = \frac{L}{RA} \tag{3}$$

where L is the thickness (mm) of the hydrogel between the two copper electrodes, A representing the contact area (mm^2) of the hydrogel and the copper electrodes. R represents the impedance, which is the intercept of the curve with the horizontal axis (Ω). The impedance of each sample was measured in triplicate.

2.7.2 Electro-mechanical properties

The electrical signal response of PVA/Pullulan/NaCl hydrogel under stretching was obtained by combining the potentiostat with a universal testing machine. The dumbbell shaped samples were clamped on the universal testing machine, and the two clamps were connected to the potentiostat. A voltage of 1 V was applied on the two ends of the hydrogel during the tensile test, and the current response was recorded. The resistance was calculated by Ohm's law. The relative resistance change was defined by **Equation 4**, and the gauge factor (GF, representing sensitivity) was calculated by determining the slope of the relative resistance change versus the applied strain according to **Equation 5**:

$$\text{Relative resistance change } (\%) = \frac{\Delta R}{R_0} \times 100 = \frac{R - R_0}{R_0} \times 100 \tag{4}$$

$$GF = \frac{d(\Delta R/R_0)}{d\varepsilon} \tag{5}$$

where R_0 is the initial resistance (Ω). R is the resistance (Ω) under tensile strain ε (%).

2.8 Human motion detection and information transmission

The PVA/Pullulan/NaCl conductive hydrogel sensors were fixed to different human joints (finger, wrist, elbow, and knee) with the aid of binder clips and tape. Both ends of the hydrogels were clamped by binder clips and connected to the potentiostat to measure the real-time variation of resistance during the movements. Additionally, the hydrogel sensors were pressed according to Morse code to realize information transmission. The authors as volunteers took part in human motion detection. A written consent is available upon request.

3. Results and Discussion

3.1 Gelation mechanism

Scheme 1 shows the hydrogel preparation mechanism. The hydrogel was prepared through the freezing-thawing process followed by the soaking method. PVA and pullulan were mixed and frozen at −20 ℃. In the freezing step, ice crystals grew among polymer chains and pushed PVA chains together. The hydroxyl groups on PVA chains formed crystalline which served as crosslinking points. In the thawing step, the ice crystals melted while the PVA crystalline remained, and the corresponding domains formed the pores surrounded by the polymer skeleton [36, 37]. Meanwhile, the hydroxyl groups of pullulan formed hydrogen bond interaction with PVA chains. Subsequently, the PVA/Pullulan hydrogel was soaked in NaCl solution at room temperature. During the soaking process, Na^+ and Cl^- ions diffused into the hydrogels and polarized the water molecules bonded with PVA. Therefore, the hydrogen bonds between water molecules and PVA were damaged and water molecules were expelled from the hydrogels [25]. Along with dehydration, the hydrogels shrank, and denser structures were formed with the aggregation of PVA. It was reported that pullulan is insensitive to NaCl [38]. Thus, we deduced that pullulan did not tend to aggregate in the hydrogel.

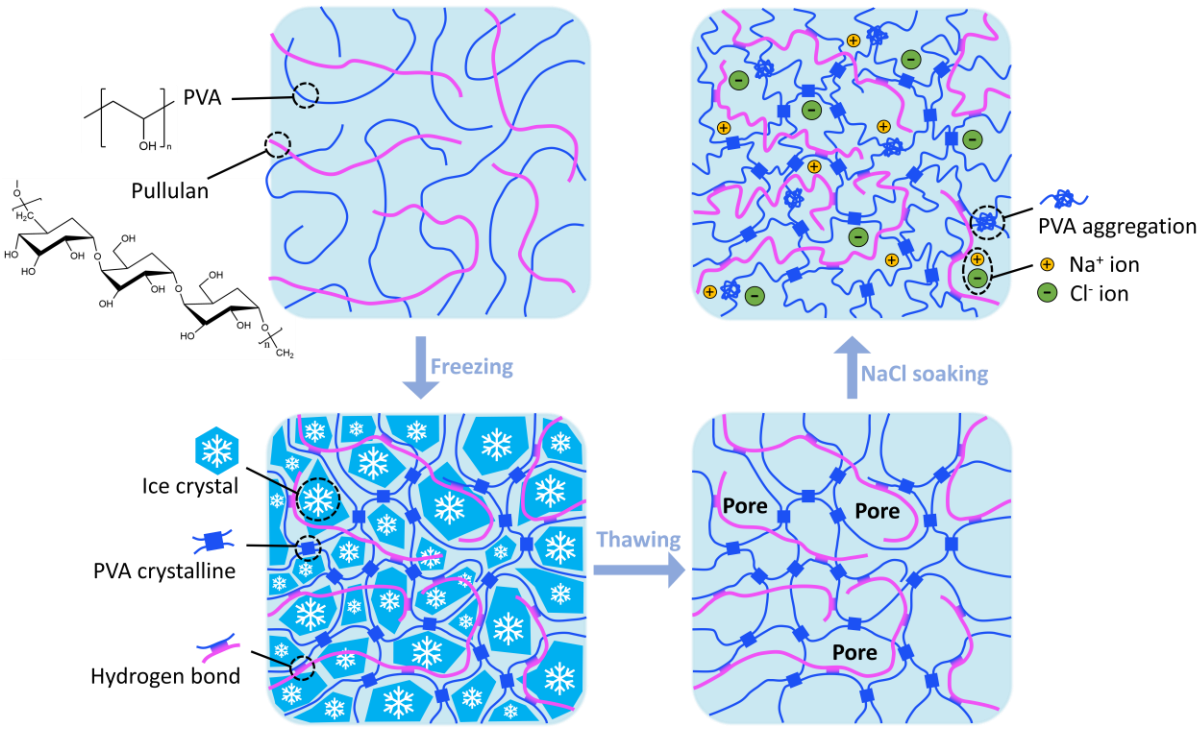

Scheme 1. Gelation mechanism of the PVA/Pullulan/NaCl ionic conductive hydrogels.

NaCl concentration had a large influence on the hydrogel size and water content (**Figure 1a–c**). At lower NaCl concentration, the hydrophilic polymer created an osmotic pressure that was higher than the NaCl solution, thus leading to a swelling [39, 40]. By contrast, reduced size and water content were obtained with higher NaCl concentration because of the salting-out effect and dehydration effect. The anions can polarize the water molecules bonded with the hydrophilic groups on polymers, thus weakening their hydrogen bonds. The polarization is more pronounced with higher salt concentrations [41-43]. Therefore, more water molecules were expelled from the hydrogels and the polymer chains aggregated at higher NaCl concentrations.

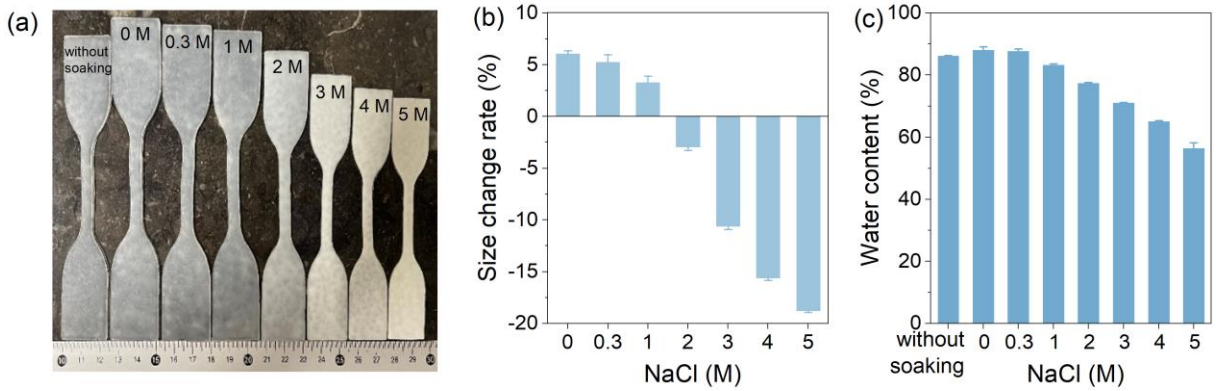

Figure 1. (a) Appearance of the hydrogels with different soaking concentrations. (b) Size change rate, and (c) water content of the $PVA_{95}/Pullulan_5/NaCl_z$ hydrogels.

3.2 Characterization of hydrogels

SEM was performed to characterize the raw materials (**Figure S2**) and observe the cross-sectional morphology of hydrogels with different magnifications (×500 and ×1000 (**Figure S3(a–g)**), ×2000 (**Figure 2a–g)**). Pure PVA hydrogel showed a dense structure. After the addition of pullulan, the structures of PVA/Pullulan hydrogels were changed. With a lower pullulan content (e.g., <5wt%), relatively intact porous networks were observed. However, the pores gradually became larger and incomplete with the increase of pullulan content (e.g., >10wt%). The white particles in Figure 3g revealed that NaCl crystals were present after soaking and the structure was very dense, indicating the occurrence of strong aggregation of the polymer chains. In addition, the existence of Na^+ and Cl^- ions was mapped from EDX elemental mapping (**Figure 2h–i**).

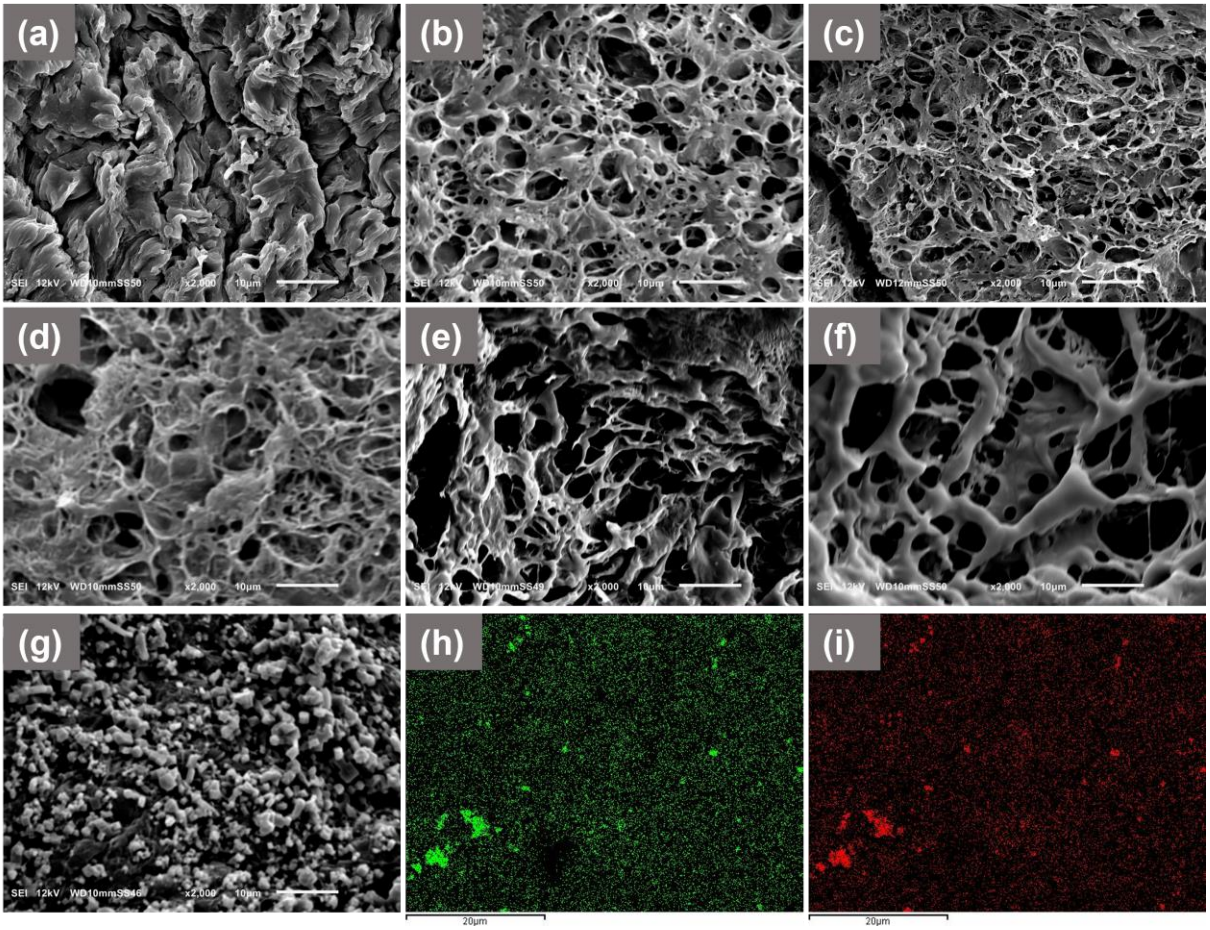

Figure 2. SEM images of (a) pure PVA hydrogel, (b) PVA_{98}/$Pullulan_2$ hydrogel, (c) PVA_{95}/$Pullulan_5$ hydrogel, (d) PVA_{90}/$Pullulan_{10}$ hydrogel, (e) PVA_{80}/$Pullulan_{20}$ hydrogel, (f) PVA_{70}/$Pullulan_{30}$ hydrogel, (g) PVA_{95}/$Pullulan_5$/$NaCl_1$ hydrogel. EDX mapping of (h) Na and (i) Cl elements for hydrogel PVA_{95}/$Pullulan_5$/$NaCl_1$.

ATR-FTIR spectroscopy was used to identify the functional groups and demonstrate the interactions of PVA and pullulan in hydrogels. **Figure 3(a)** presented the ATR-FTIR spectra of PVA, pullulan, PVA/Pullulan hydrogels and PVA/Pullulan/NaCl hydrogels. Regarding the spectrum of pullulan, a broad band at 3309 cm^{-1} was shown corresponding to –OH stretch vibration, which is a typical polysaccharide peak [44]. In the case of PVA,

the broad band at 3278 cm^{-1} was due to the stretching of hydrogen-bonded hydroxyl groups [45, 46]. For pure PVA hydrogel, the vibration of the –OH groups slightly shifted to a lower wavenumber in comparison to raw PVA, proving that hydrogen bonds were formed during the freezing-thawing process. It was found that the hydrogen bond peaks were present in all PVA/pullulan hydrogels, and these peaks shifted to lower frequencies relative to pure PVA hydrogel. This indicated the existence of stronger hydrogen bond interactions between PVA and pullulan [32, 46]. After soaking in 1 M NaCl solution, the hydrogel showed weak intensity. It was inferred that the hydrogen bond reflection was hidden by NaCl crystals. To sum up, the ATR-FTIR validated the hydrogen bond formation in the hydrogels.

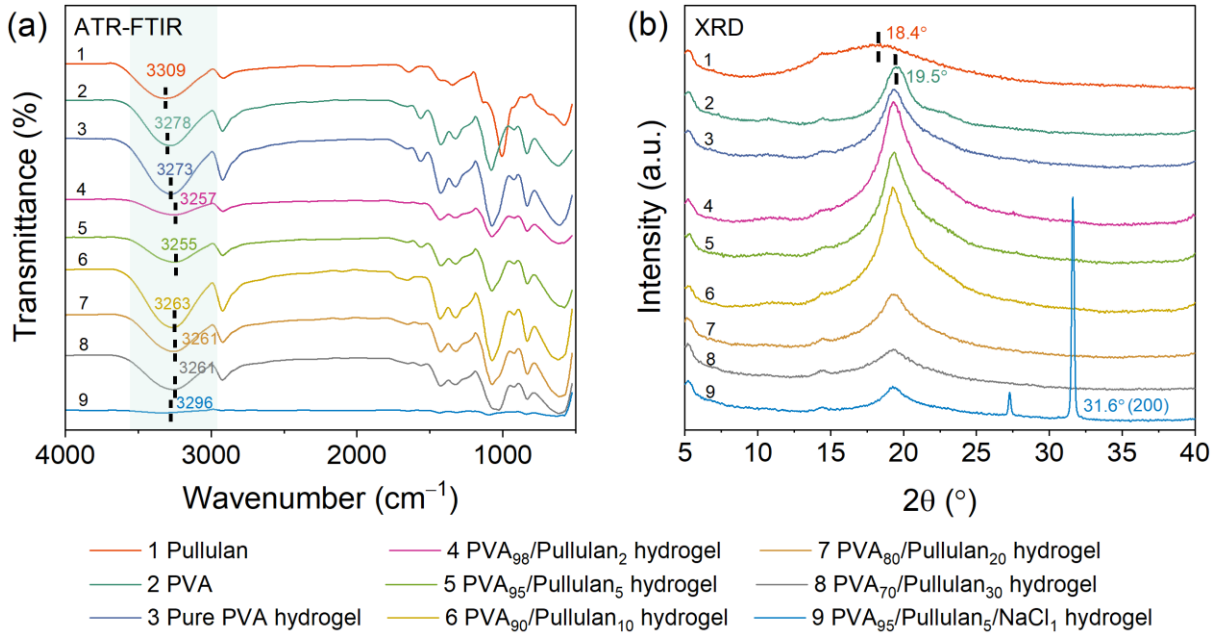

Figure 3. (a) ATR-FTIR spectra, and (b) XRD pattern of pullulan, PVA, PVA_x/$Pullulan_y$ hydrogels and PVA_{95}/$Pullulan_5$/$NaCl_1$ hydrogels.

XRD was carried out to characterize the crystal structures of Pullulan, PVA, PVA_x/$Pullulan_y$ hydrogels and PVA_{95}/$Pullulan_5$/$NaCl_1$ hydrogel (**Figure 3(b)**). The XRD pattern of pullulan showed a broad peak around 2θ = 18.4°, implying the amorphous nature. The PVA pattern displayed the typical diffraction peak at 2θ = 19.5° (101), reflecting the crystalline structure. For PVA/Pullulan hydrogels, all samples presented diffraction peaks near 2θ = 19.5°. The diffraction peaks gradually became broader, and the intensity decreased with higher pullulan content. This phenomenon was associated with the fact that the crystallite formation of PVA was interfered with higher pullulan content. After soaking in 1 M NaCl solution, a sharp diffraction peak at 2θ = 31.6° was detected. This was assigned to the (200) plane of NaCl (PDF card 5–628) [47], which demonstrated the presence of crystallized NaCl in the hydrogel.

The freezing point of the hydrogels was investigated by DSC (**Figure S4**). The exothermic peak shifted to lower temperatures with higher NaCl concentration. Na^+ and Cl^- dissolved between the water molecules and disrupted the water molecules to form a regular crystal structure. Due to the colligative properties of a solution, the freezing point of the hydrogels dropped further as the NaCl concentration increased.

3.3 Mechanical properties

The mechanical properties of the PVA_x/$Pullulan_y$ hydrogels, PVA_{95}/$Pullulan_5$/$NaCl_z$ hydrogels and PVA_{100}/$NaCl_z$ hydrogels were investigated. **Figure 4(a–d)** displayed the tensile stress-strain curves and mechanical performances of PVA/Pullulan hydrogels. Compared with pure PVA hydrogel, PVA/Pullulan hydrogels showed enhanced mechanical performances. The highest tensile strength and Young's modulus were achieved at 5wt% pullulan content and with values of 0.50 MPa and 0.07 MPa, respectively, which were 2.17 and 1.75-fold higher than those of pure PVA hydrogel. With the increase of pullulan contents (e.g., >10wt%), the amount of PVA decreased correspondingly, leading to weak and incomplete hydrogel network structures, and thus tensile strength decreased. The tensile strain of PVA/Pullulan hydrogels exhibited similar values, but the toughness enhanced from 0.16 MJ/m^3 for pure PVA hydrogel to 0.38 MJ/m^3 for PVA_{98}/$Pullulan_2$ hydrogel. These results indicated that PVA/Pullulan hydrogels were more resistant to external tensile stress in comparison to pure PVA hydrogels. This significant enhancement of the mechanical properties can be attributed to the energy dissipation of PVA/Pullulan hydrogels [48]. Pullulan was incorporated into the PVA network to form hydrogen bonds and chain entanglements with PVA. The hydrogen bonds between pullulan and PVA could break to relax the stress. On the other hand, the entanglements functioned as slip links [49]. The tensile stress was transmitted along the pullulan chains or transferred to PVA chains through the entanglements. When the pullulan chains were stretched to the maximum length and break, the tensile stress was dissipated. Therefore, the hydrogen bonds and the physical entanglements played sacrificial roles to dissipate energy and enhance mechanical properties. We concluded that suitable amounts of pullulan brought remarkable enhancement in mechanical properties, and hydrogel with 5wt% pullulan content can be chosen as a representative of the hydrogels.

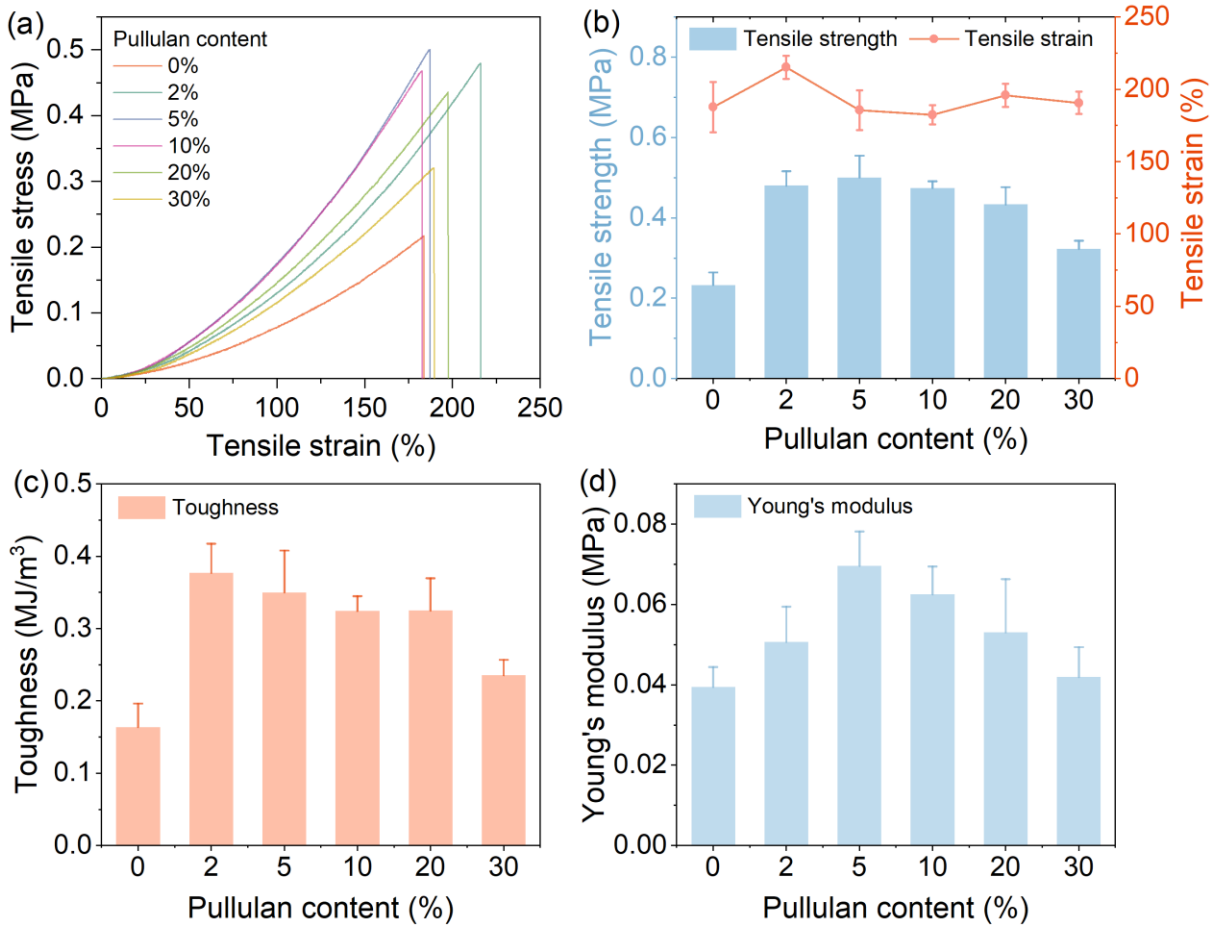

Figure. 4. Mechanical properties of the PVA_x/$Pullulan_y$ hydrogels, including (a) tensile stress-strain curves, (b) tensile strength and tensile strain, (c) toughness and (d) Young's modulus.

Subsequently, PVA_{95}/$Pullulan_5$ hydrogels were soaked in NaCl solution (0–5 M) and the mechanical properties were evaluated. **Figure 5(a–d)** intuitively presented the mechanical properties. The hydrogels could be stretched, rolled, twisted, and were able to withstand heavy objects. The tensile tests (**Figure 5(e–h)**) showed that the mechanical properties of PVA_{95}/$Pullulan_5$/$NaCl_z$ hydrogels can be tuned by adjusting the NaCl concentration (0–5 M). As the NaCl concentration increased, the tensile strength, toughness and Young's modulus increased progressively and reached the highest values of 2.72 MPa, 2.90 MJ/m^3 and 1.49 MPa at 5 M, respectively, which were 5.44, 8.29 and 21.29-fold higher than those of PVA/Pullulan hydrogel without soaking. Moreover, the PVA/Pullulan/NaCl hydrogels had enhanced stretchability compared with the hydrogels without soaking (**Figure 5(f)**). The highest stretchability was 1.33 times that of pure PVA hydrogel. This significant enhancement resulted from the change in the polymer configuration and water content. During the salting-out process, the aggregation occurred and the configuration of PVA and pullulan chains was rearranged, which served as the "crosslinking" points in the hydrogels. Water is considered as a plasticizer that interacts with the polymers, and polymer-polymer interaction is weakened if much water exists inside hydrogels. Thus, mechanical enhancement happened due to the reinforced polymer-polymer interaction arising from the loss of water [39]. To demonstrate the synergy of pullulan and salting-out effect, we evaluated the mechanical properties of

PVA/NaCl hydrogels as a comparison (**Figure S5**). We found that PVA/Pullulan/NaCl hydrogel possessed significant mechanical improvement in comparison with pure PVA hydrogels, PVA/Pullulan hydrogels, and PVA/NaCl hydrogels. These results verified that the pronounced enhancement of the mechanical performances was ascribed to the synergy between pullulan and salting-out effect. Moreover, the hydrogels covered a large range of Young's modulus from 0.07 MPa to 1.49 MPa, which was comparable to that of certain human tissues and PDMS [50-54] (**Figure S6)**. Beneficial from the mechanical strength, stretchability, and skin-like Young's modulus, the resultant hydrogels had potential in wearable sensors.

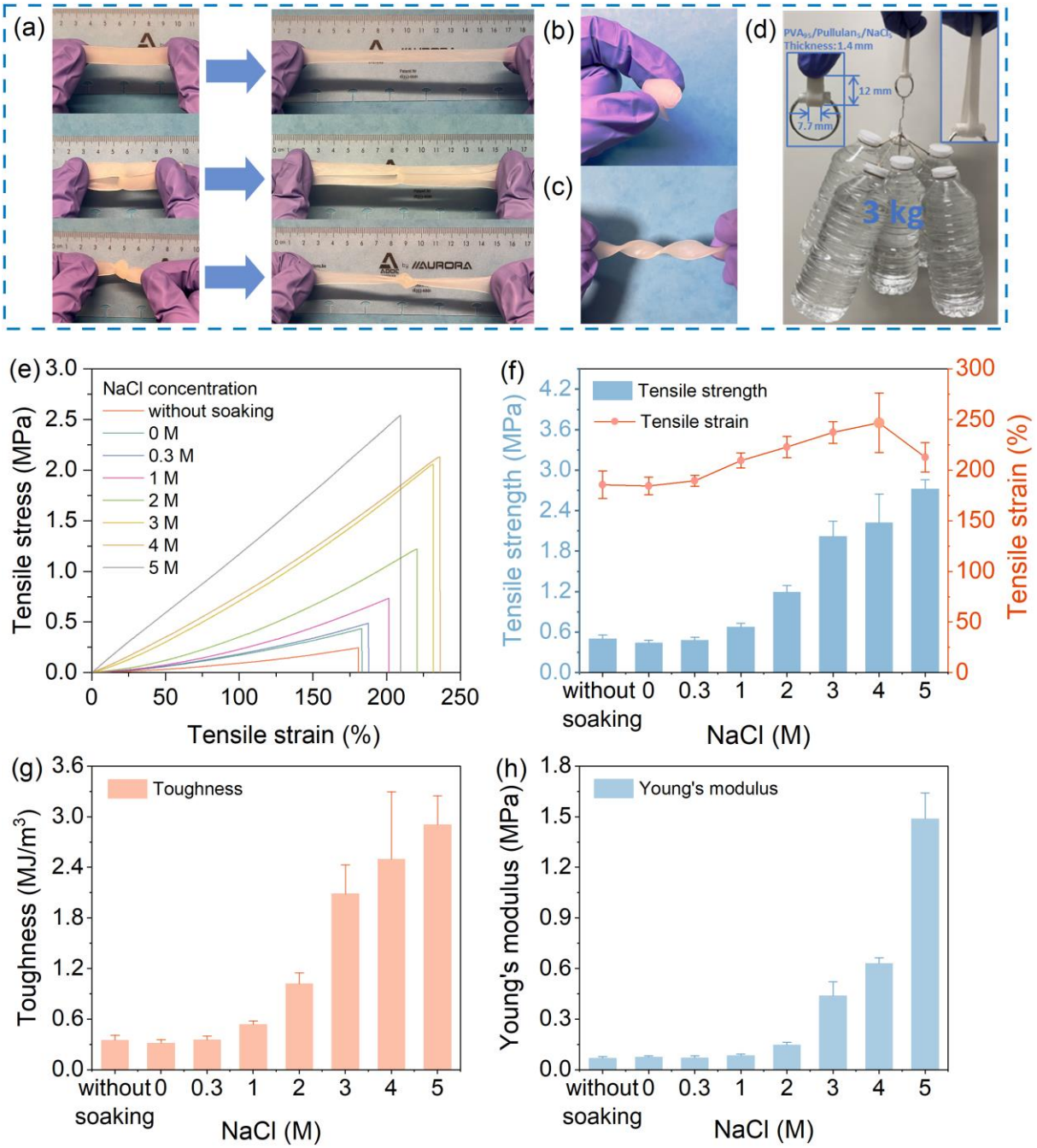

Figure 5. (a) Stretching, (b) rolling, and (c) twisting of the $PVA_{95}/Pullulan_5/NaCl_1$ hydrogels. (d) Load-bearing illustration of $PVA_{95}/Pullulan_5/NaCl_5$ hydrogel. (e) Tensile stress-strain curves, (f) tensile strength and tensile strain, (g) toughness and Young's modulus of the $PVA_{95}/Pullulan_5/NaCl_z$ hydrogels.

Successive cyclic loading-unloading tests were performed to evaluate the energy dissipation behaviour of $PVA_{95}/Pullulan_5/NaCl_1$ hydrogels. Specimens were stretched to different maximum tensile strains (40%, 60%, 80%) and returned to the initial state. **Figure 6(a)** presented the hysteresis loops of the first cycle at different maximum tensile strains. Under the 40% tensile strain, the loading-unloading curves almost coincided. The hydrogel exhibited negligible dissipated energy of 0.47 kJ/m^3 (**Figure 6(b)**), indicating that the hydrogel can self-recover under small strain. With the increase of tensile strain to 60% and 80%, hysteresis was observed, and the dissipated energy increased to 3.10 kJ/m^3 and 8.96 kJ/m^3, respectively. This indicated that the energy was dissipated at large tensile strain, which was ascribed to the destruction of the hydrogen bonds between PVA and pullulan, and the friction of the molecular chains [55]. Afterwards, the cyclic loading-unloading test was performed at the tensile strain of 60% to investigate the energy dissipation behaviour in the long term. The hydrogel showed a pronounced hysteresis loop only in the first cycle while the later cycles were much smaller with decreased dissipated energy (**Figure 6(c–d)**). This was because of the permanent fracture of the hydrogen bonds in the first cycle [56].

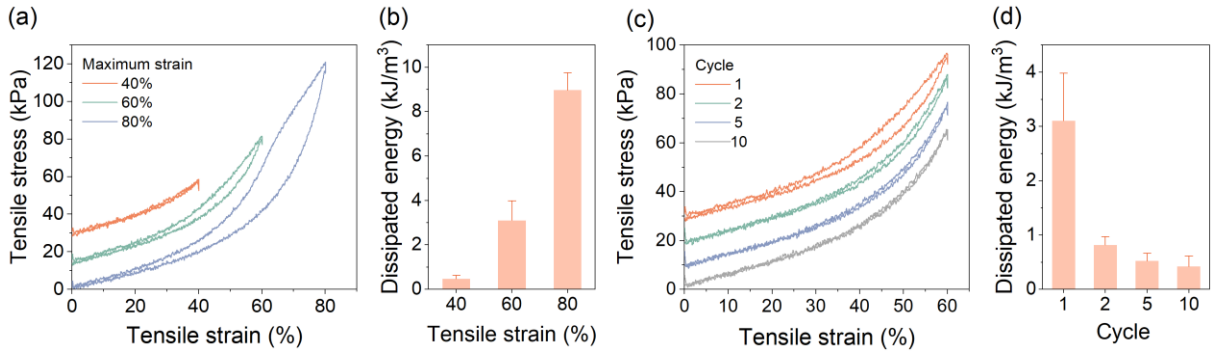

Figure 6. Successive cyclic tensile loading-unloading performances of the $PVA_{95}/Pullulan_5/NaCl_1$ hydrogels at (a) different maximum tensile strains, and (b) the corresponding dissipated energy. (c) Ten cycles of successive cyclic loading-unloading curves of the $PVA_{95}/Pullulan_5/NaCl_1$ hydrogel at the strain of 60% and (d) the corresponding dissipated energy.3.5 Electrical property and sensing performance

The hydrogels were ionic conductive due to the presence of Na^+ and Cl^- ions. Under an electric field, the Na^+ and Cl^- ions moved oppositely in the hydrogel matrix leading to the occurrence of electric current [57]. The EIS spectra of the hydrogels were presented in **Figure 7(a–b)**. The hydrogels exhibited evident ionic conductivity after soaking in NaCl solutions (**Figure 7(c)**). The ionic conductivity went up with increasing NaCl soaking concentrations since more ions were present in the hydrogels. However, less conductivity was induced at the concentration of 5 M because the ions formed ion clusters, reducing the number of charge carriers [58]. Notably, at a concentration of 4 M, the ionic conductivity was as high as 10.44 S m^{-1}, which was 25.46 folder than hydrogel without soaking.

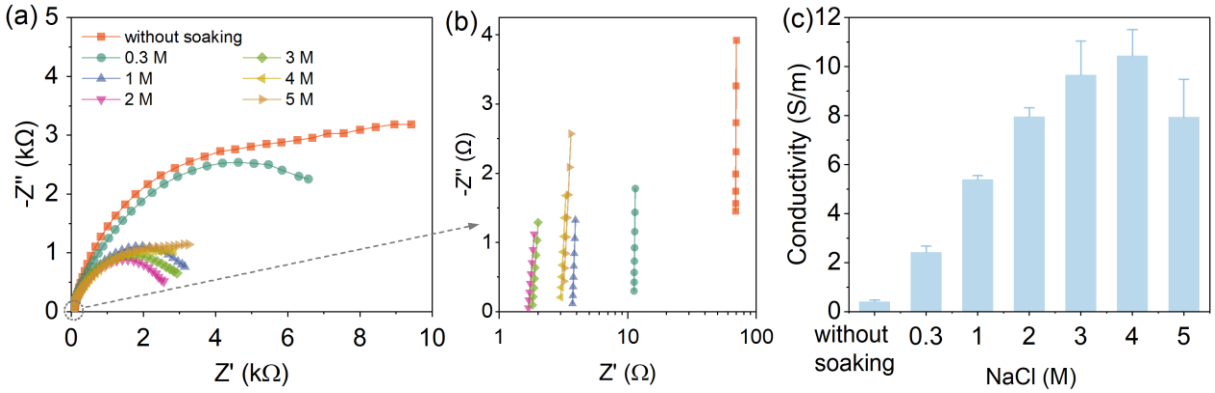

Figure 7. (a) EIS spectra of the PVA/Pullulan/$NaCl_z$ hydrogels. (b) Zoom in on the resistance of 0–100 Ω. (c) Ionic conductivity of the PVA/Pullulan/$NaCl_z$ hydrogels.

Subsequently, the relative resistance changes with strain and sensitivity were studied, with a setup shown in **Figure 8(a)**. The specimen was connected to a potentiostat on both ends. By applying a voltage of 1 V, the change of electrical signals was recorded during the tensile test. The results showed that the relative resistance changes increased with the increase of applied strain (**Figure 8(b)**), and the relationship could be fitted with the polynomial equation $y = A\,\varepsilon^2 + B\,\varepsilon + C$, where y was the relative resistance change, and $\boldsymbol{\varepsilon}$ was the tensile strain. The gauge factor (GF) is represented by the tangent slope of the relative resistance change. GF in this work could be expressed as $GF = 2A\,\varepsilon + B$, indicating that the GF linearly changed with the applied strain (**Figure 8(c)**). This was because the resistance increased due to the geometric effect. And higher GF was achieved at lower NaCl concentration since more loose structures were formed due to slight swelling, which caused large structure deformation and resulted in larger resistance change. In comparison with many other similar PVA ionic hydrogel sensors (**Table S2**), our hydrogels showed high sensitivity. We attributed this to the aggregated structures because of the salting-out effect. Under stretching, the aggregated polymers were stretched to a relaxed state, which contributed to the large geometric effect and brought a higher GF.

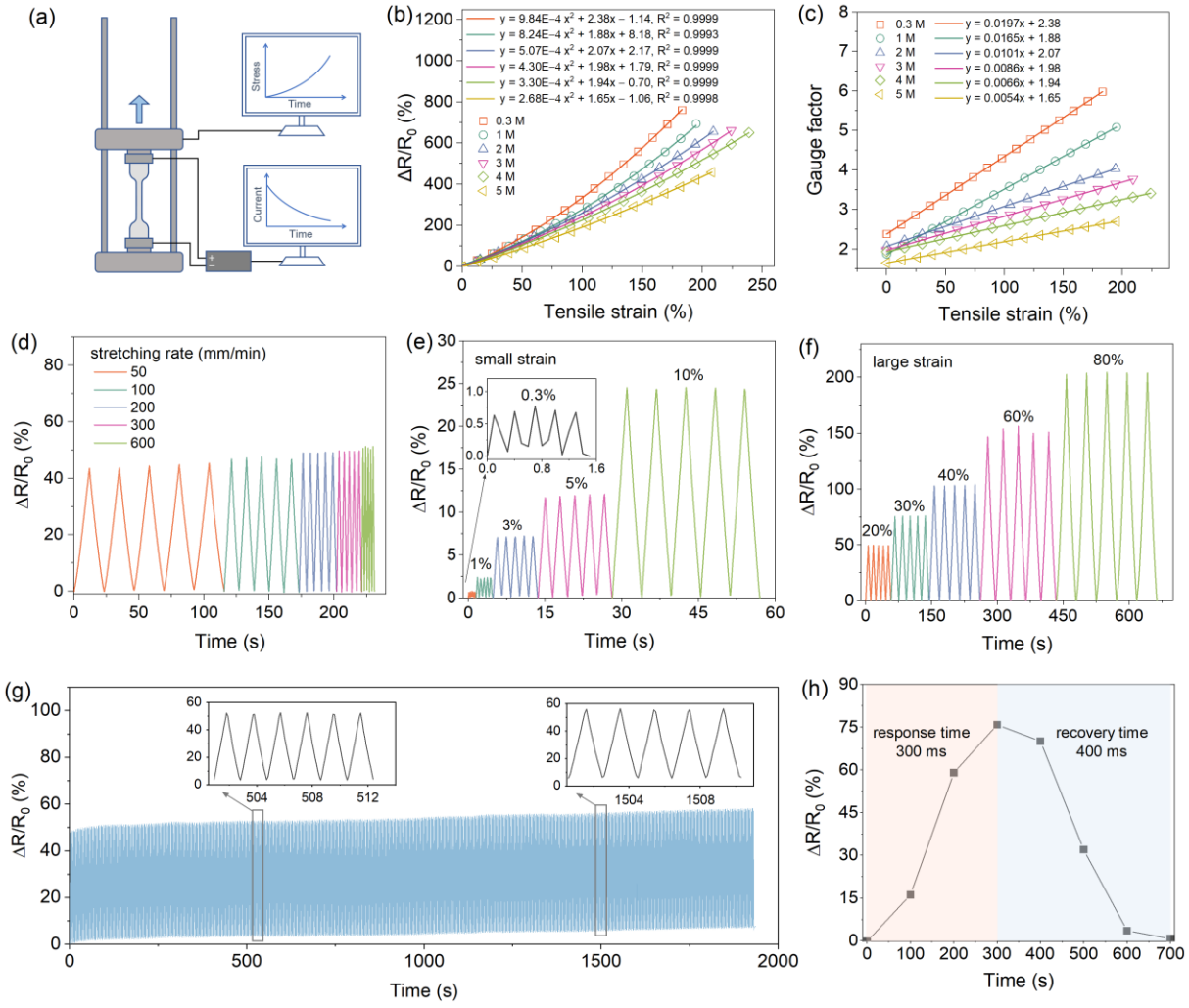

Figure 8. Sensing performance of the PVA/Pullulan/NaCl hydrogels: (a) Schematic diagram of the sensing tests. (b) The relative resistance changes of the $PVA_{95}/Pullulan_5/NaCl_z$ hydrogels as a function of tensile strain. (c) Gauge factor with various NaCl concentrations and tensile strains. Sensing performance of the $PVA_{95}/Pullulan_5/NaCl_1$ hydrogel: (d) Relative resistance changes at 20% of strain with different stretching rates. Electrical signal responses under cyclic loading−unloading at (e) small strains and (f) large strains. (g) The durability test at a strain of 20% for 1000 cycles. (h) Response time and recovery time, extracted from the electrical signals of finger bending.

As a trade-off between water content, mechanical performances, sensitivity, and the NaCl soaking concentration, $PVA_{95}/Pullulan_5/NaCl_1$ conductive hydrogel was selected as an example to evaluate the sensing performance. The hydrogel sensor responded stably at different stretching rates (50–600 mm/min) (**Figure 8(d)**), suggesting its high applicability in real conditions. **Figure 8(e–g)** showed the change of relative resistance at different strains. When the hydrogel sensor was cyclically stretched, the relative resistance changed reversibly. In the loading-unloading cycles, the hydrogel sensors produced almost perfectly symmetrical peaks at all strains (0.3%–80%). The stepwise change of the relative resistance indicated that the hydrogel sensors could recognize various strains and produced steady, and repeatable resistance signals. Then, the cyclic loading-unloading test at 20% strain was performed to evaluate the durability (**Figure 8(g)**). The hydrogel had close signal responses at 500 s and 1500 s, with an acceptable signal drift

after 1000 cycles [59-61]. Additionally, by analyzing the electrical response of finger joint movement, we found that the hydrogel sensor possessed a response time of 300 ms and a recovery time of 400 ms (**Figure 8(h)**). These results indicate that the PVA_{95}/$pullulan_5$/$NaCl_1$ hydrogel sensor is a potential candidate in wearable strain sensors.

3.4 Real-time detection of human motions

As proof of concept, PVA_{95}/$Pullulan_5$/$NaCl_1$ hydrogels were assembled into strain sensors for human motion detection (**Figure 9(a–f)**). From **Figure 9(b)**, the relative resistance changed stepwise with larger bending angles. **Figure 9(c–f)** depicted the relative resistance change during the bending-unbending of the different joints (finger, wrist, elbow, and knee). The hydrogel sensors can generate reproducible and stable electrical signals, proving the reliability of the hydrogel sensor in monitoring joint movement. Besides, the electrical signals were reversible during the bending-unbending. A practical basketball sports monitoring system was shown in **Movie S1**. The good sensing performance demonstrates that the PVA/Pullulan/NaCl hydrogel sensor is promising in scenarios that require real-time monitoring and visual feedback, such as rehabilitation or sports training.

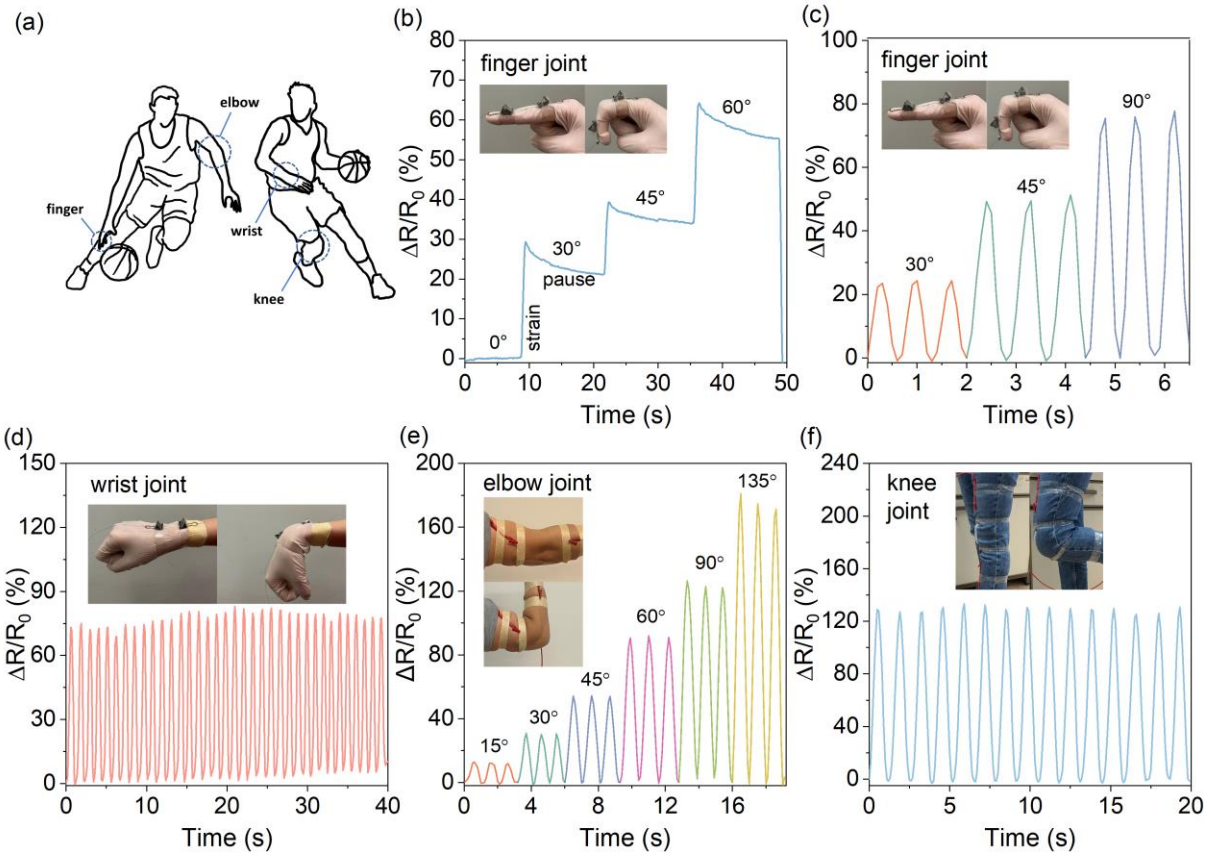

Figure 9. Application of the selected PVA/Pullulan/NaCl hydrogel as strain sensor. (a) Sensing test at different human joints. (b) The relative resistance changes of finger movement at different angles with a pause. The real-time monitoring of continuous joint motions of (c) finger, (d) wrist (e) elbow, (f) knee.

3.5 Information communication through Morse code

Apart from its application as a strain sensor for human motion detection, the PVA_{95}/$Pullulan_5$/$NaCl_1$ conductive hydrogel was also explored for information communication through Morse code. Morse code has been internationally recognized as a tool for information encryption and decryption. It is used for information communication in some special situations. On one hand, different words, punctuations, numbers, or sentences can be translated by a combination of “dots” and “dashes”. On the other hand, the relative resistance of the PVA/Pullulan/NaCl conductive hydrogels changed synchronously with the deformation.

Figure 10(a–b) displayed the creation of Morse code signals. When the hydrogel sensor was pressed with different durations, it generated different electrical signals corresponding to the “dot” and “dash” of the Morse code. The electrical signal with a sharp peak induced by short pressing represented a “dot”, and the signal with a straight line resulting from long pressing represented a “dash”. Based on the Morse code, we showcased words such as “MORSE”, “CODE”, “HELP”, and “SOS” (**Figure 10(c–f)**). The electrical signal outputs were repeatable, which demonstrated the feasibility of the PVA/Pullulan/NaCl conductive hydrogels to transmit information using Morse code. This silent way of information communication is of practical significance, such as for emergency rescues where direct calling for help is not applicable or information communication for blind people.

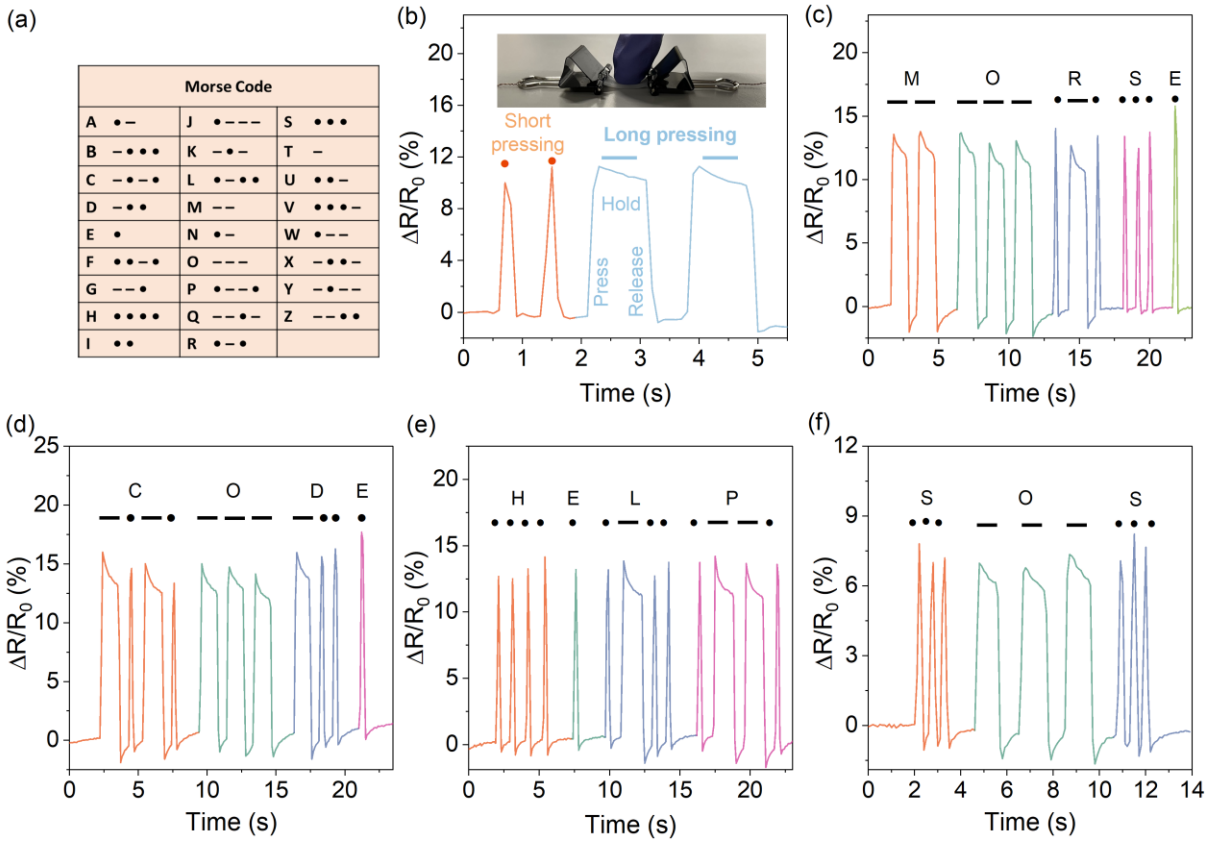

Figure 10. (a) The corresponding alphabet of Morse code. (b) Generation of Morse code signals by pressing hydrogels. Demonstration of PVA/Pullulan/NaCl hydrogel sending messages through Morse code: (c) MORSE, (d) CODE, (e) HELP, (f) SOS.

4. Conclusions

In this work, PVA/Pullulan/NaCl ionic conductive hydrogels with enhanced mechanical strength, superior ionic conductivity, and high sensitivity have been developed by the combination of freezing-thawing and soaking process. The semi-interpenetrating network between pullulan and PVA together with the salting-out effect facilitated the improvement of mechanical strength (up to 2.72 MPa). The presence of ions (Na^+, Cl^-) endowed the hydrogels with high conductivity (10.44 S/m) and high sensitivity (GF up to 5.98). The ionic hydrogel can realize the detection of joint movements and information transmission through Morse code. This ionic conductive hydrogel sensor exhibits balanced overall merits, showing the potential applications in wearable sensors. Beyond this, due to the high mechanical strength and ionic conductivity, this ionic hydrogel is potentially expanded as wearable flexible supercapacitors, unlocking versatile wearable applications. We envision this hydrogel strain sensor offers a promising and sustainable solution to wearable electronics.

Supporting Information

- Additional experiments details and results, including composition of the hydrogels, comparison of mechanical properties and gauge factor with other similar work, molecular distribution of pullulan, SEM of the raw materials and hydrogels, DSC of PVA_{95}/$Pullulan_5$/$NaCl_z$ hydrogels, mechanical properties of PVA/NaCl hydrogels, Young's modulus comparison of PVA/Pullulan/NaCl hydrogels with human tissues and common traditional materials in stretchable electronics (PDF)
- Movie S1: Basketball Illustration (mp4)

Data Availability Statement

The data that support the findings of this research are available from the corresponding author upon reasonable request.

Author Contributions

The manuscript was written through contributions of all authors. All authors have given approval to the final version of the manuscript.

Conflict of Interest Disclosure

The authors declare no competing financial interest.

Acknowledgements

The authors thank Bernard Appeltans (Drug Delivery and Disposition, KU Leuven), Femke De Ceulaer (Department of Chemical Engineering, KU Leuven), Hao-qun Qiu (Department of Chemical Engineering, KU Leuven) and Filippo Franceschini (Department

of Physics and Astronomy, KU Leuven) for technical assistance. The authors thank Prof. Francisco Molina-Lopez (Department of Materials Engineering, KU Leuven) for fruitful discussions. The China Scholarship Council Funding is acknowledged for its support.

References

1. Molina-Lopez, F. Emerging thermoelectric generators based on printed and flexible electronics technology. In *2020 IEEE SENSORS*. Rotterdam, Netherlands, October 25-28, 2020.IEEE.
2. Liu, H., et al., Spatially modulated stiffness on hydrogels for soft and stretchable integrated electronics, *Mater. Horiz.*, 2020, 7, 1, 203-213. 10.1039/C9MH01211G
3. Zhang, D., et al., Highly stretchable, self-adhesive, biocompatible, conductive hydrogels as fully polymeric strain sensors, *J. Mater. Chem. A*., 2020, 8, 39, 20474-20485. 10.1039/D0TA07390C
4. Park, S., et al., Three-dimensional self-healable touch sensing artificial sin device, *ACS Appl. Mater. Interfaces*, 2020, 12, 3, 3953-3960. 10.1021/acsami.9b19272
5. Leng, Z.W., et al., Sebum-membrane-inspired protein-based bioprotonic hydrogel for artificial skin and human-machine merging interface, *Adv. Funct. Mater.*, 2023, 33, 13, 2211056. 10.1002/adfm.202211056
6. Hu, O., et al., An Antifreezing, Tough, Rehydratable, and Thermoplastic Poly(vinyl alcohol)/Sodium Alginate/Poly(ethylene glycol) Organohydrogel Electrolyte for Flexible Supercapacitors, *ACS Sustainable Chem. Eng.*, 2021, 9, 29, 9833-9845. 10.1021/acssuschemeng.1c02464
7. Ge, W., et al., Nanocellulose/LiCl systems enable conductive and stretchable electrolyte hydrogels with tolerance to dehydration and extreme cold conditions, *Chem. Eng. J.*, 2021, 408, 127306. https://doi.org/10.1016/j.cej.2020.127306
8. Shu, L., et al., Facile fabrication of strong and conductive cellulose hydrogels with wide temperature tolerance for flexible sensors, *Int. J. Biol. Macromol.*, 2023, 240, 124438. https://doi.org/10.1016/j.ijbiomac.2023.124438
9. Zeng, L., B. Liu, and G. Gao, Physically crosslinked polyvinyl alcohol/chitosan-phytic acid hydrogels for wearable sensors with highly conductive, recyclable and antibacterial properties, *Sci. China Mater.*, 2023, 66, 4062-4070. 10.1007/s40843-023-2530-4
10. Xia, S., et al., Recyclable hydrogel for human-machine interface of multi-mode human vital signal acquisition, *Sci. China Mater.*, 2023, 66, 7, 2843-2851. 10.1007/s40843-022-2411-9
11. Chen, G., et al., Highly tough supramolecular double network hydrogel electrolytes for an artificial flexible and low-temperature tolerant sensor, *J. Mater. Chem. A*., 2020, 8, 14, 6776-6784. 10.1039/D0TA00002G
12. Xing, W. and Y. Tang, On mechanical properties of nanocomposite hydrogels: Searching for superior properties, *Nano Mater. Sci.*, 2022, 4, 2, 83-96. https://doi.org/10.1016/j.nanoms.2021.07.004
13. Ye, Y., et al., Cellulose nanofibrils enhanced, strong, stretchable, freezing-tolerant ionic conductive organohydrogel for multi-functional sensors, *Adv. Funct. Mater.*, 2020, 30, 35, 2003430. https://doi.org/10.1002/adfm.202003430
14. *ECHA*. https://echa.europa.eu/information-on-chemicals (accessed 1-February-2024).
15. Fredricks, J.L., et al., Hierarchical biopolymer-based materials and composites, *J. Polym Sci.*, 2023, 61, 21, 2585-2632. https://doi.org/10.1002/pol.20230126
16. Yan, M., et al., Anisotropic Muscle-like Conductive Composite Hydrogel Reinforced by Lignin and Cellulose Nanofibrils, *ACS Sustainable Chem. Eng.*, 2022, 10, 39, 12993-13003. 10.1021/acssuschemeng.2c02506
17. Dodda, J.M., et al., Biocompatible hydrogels based on chitosan, cellulose/starch, PVA and PEDOT:PSS with high flexibility and high mechanical strength, *Cellulose*, 2022, 29, 12, 6697-6717. 10.1007/s10570-022-04686-4
18. Zhang, R., et al., Alginate Fiber-Enhanced Poly(vinyl alcohol) Hydrogels with Superior Lubricating Property and Biocompatibility, *Polymers*, 2022, 14, 19. 10.3390/polym14194063
19. Wang, Z., et al., Naturally sourced hydrogels: emerging fundamental materials for next-generation healthcare sensing, *Chem. Soc. Rev.*, 2023, 52, 9, 2992-3034. 10.1039/D2CS00813K

20. Nasrollahzadeh, M., et al., *Chapter 2 - Polysaccharides in food industry*, in *Biopolymer-Based Metal Nanoparticle Chemistry for Sustainable Applications*, M. Nasrollahzadeh, 2021, Elsevier. 47-96.
21. Teramoto, N., et al., Morphology and mechanical properties of pullulan/poly(vinyl alcohol) blends crosslinked with glyoxal, *J. Appl. Polym. Sci.*, 2001, 82, 9, 2273-2280. https://doi.org/10.1002/app.2075
22. Soni, S.R. and A. Ghosh, Exploring pullulan-poly(vinyl alcohol) interpenetrating network microspheres as controlled release drug delivery device, *Carbohydr. Polym.*, 2017, 174, 812-822. https://doi.org/10.1016/j.carbpol.2017.07.016
23. Samoila, I., et al., Pullulan/Poly(Vinyl Alcohol) Composite Hydrogels for Adipose Tissue Engineering, *Materials*, **2019**. 12, 19, 3220. 10.3390/ma12193220
24. Plugariu, I.-A., et al., Poly(vinyl alcohol)/Pullulan Composite Hydrogels as a Potential Platform for Wound Dressing Applications, *Gels*, 2023, 9, 7, 580. 10.3390/gels9070580
25. Wu, S., et al., Poly(vinyl alcohol) hydrogels with broad-range tunable mechanical properties via the hofmeister effect, *Adv. Mater.*, 2021, 33, 11, 2007829. https://doi.org/10.1002/adma.202007829
26. Zhang, Y. and P.S. Cremer, Interactions between macromolecules and ions: the Hofmeister series, *Curr. Opin. Chem. Biol.*, 2006, 10, 658-663. https://doi.org/10.1016/j.cbpa.2006.09.020
27. Kuang, X., et al., Functional tough hydrogels: Design, processing, and biomedical applications, *Acc. Mater. Res.* , 2023, 4, 2, 101-114. 10.1021/accountsmr.2c00026
28. Görgényi, M., et al., Aqueous salting-out effect of inorganic cations and anions on non-electrolytes, *Chemosphere*, 2006, 65, 5, 802-810. https://doi.org/10.1016/j.chemosphere.2006.03.029
29. Ye, W., et al., High strength, anti-freezing, and conductive poly(vinyl alcohol)/urea ionic hydrogels as soft sensor, *Polym. Eng. Sci.*, 2022, 62, 12, 3985-3993. https://doi.org/10.1002/pen.26160
30. Zhang, L., et al., Super strong and tough anisotropic hydrogels through synergy of directional freeze-casting, metal complexation and salting out, *Chem. Eng. J.*, 2023, 463, 142414. https://doi.org/10.1016/j.cej.2023.142414
31. Zhou, Y., et al., Highly stretchable, elastic, and ionic conductive hydrogel for artificial soft electronics, *Adv. Funct. Mater.*, 2019, 29, 1, 1806220. https://doi.org/10.1002/adfm.201806220
32. Hu, J., et al., One-pot freezing-thawing preparation of cellulose nanofibrils reinforced polyvinyl alcohol based ionic hydrogel strain sensor for human motion monitoring, *Carbohydr. Polym.*, 2022, 275, 118697. https://doi.org/10.1016/j.carbpol.2021.118697
33. Dong, X., et al., Strong and Tough Conductive Organo-Hydrogels via Freeze-Casting Assisted Solution Substitution, *Adv. Funct. Mater.*, 2022, 32, 31, 2203610. https://doi.org/10.1002/adfm.202203610
34. Xiang, C., et al., A self-reinforced tough and multifunctional polyvinyl alcohol fabric composite hydrogel, *Compos. Sci. Technol.*, 2023, 243, 110212. https://doi.org/10.1016/j.compscitech.2023.110212
35. Liu, X., et al., Robust conductive organohydrogel strain sensors with wide range linear sensing, UV filtering, anti-freezing and water-retention properties, *Colloids Surf. A Physicochem. Eng. Asp.*, 2022, 632, 127823. https://doi.org/10.1016/j.colsurfa.2021.127823
36. Yokoyama, F., et al., Morphology and structure of highly elastic poly(vinyl alcohol) hydrogel prepared by repeated freezing-and-melting, *Colloid. Polym. Sci.*, 1986, 264, 595-601. 10.1007/BF01412597
37. Abitbol, T., et al., Reinforcement with cellulose nanocrystals of poly(vinyl alcohol) hydrogels prepared by cyclic freezing and thawing, *Soft Matter*, 2011, 7, 2373-2379. 10.1039/C0SM01172J
38. Kumar, R., et al., A high-throughput method for Illumina RNA-Seq library preparation, *Front. Plant Sci.*, 2012, 3. 10.3389/fpls.2012.00202
39. Cui, W., et al., Strong tough conductive hydrogels via the synergy of ion-induced cross-linking and salting-out, *Adv. Funct. Mater.*, 2022, 32, 39, 2204823. https://doi.org/10.1002/adfm.202204823
40. Buenger, D., F. Topuz, and J. Groll, Hydrogels in sensing applications, *Prog. Polym. Sci.*, 2012, 37, 12, 1678-1719. https://doi.org/10.1016/j.progpolymsci.2012.09.001
41. Muta, H., M. Miwa, and M. Satoh, Ion-specific swelling of hydrophilic polymer gels, *Polymer*, 2001, 42, 14, 6313-6316. https://doi.org/10.1016/S0032-3861(01)00098-2
42. Zhang, Y., et al., Specific ion effects on the water solubility of macromolecules: PNIPAM and the hofmeister series, *J. Am. Chem. Soc.*, 2005, 127, 41, 14505-14510. 10.1021/ja0546424

43. Zhang, Y. and P.S. Cremer, Interactions between macromolecules and ions: the Hofmeister series, *Curr. Opin. Chem. Biol.*, 2006, 10, 6, 658-663. https://doi.org/10.1016/j.cbpa.2006.09.020
44. Coseri, S., et al., Green synthesis of the silver nanoparticles mediated by pullulan and 6-carboxypullulan, *Carbohydr. Polym.*, 2015, 116, 9-17. https://doi.org/10.1016/j.carbpol.2014.06.008
45. Mansur, H.S., R.L. Oréfice, and A.A.P. Mansur, Characterization of poly(vinyl alcohol)/poly(ethylene glycol) hydrogels and PVA-derived hybrids by small-angle X-ray scattering and FTIR spectroscopy, *Polymer*, 2004, 45, 21, 7193-7202. https://doi.org/10.1016/j.polymer.2004.08.036
46. Coates, J., *Interpretation of Infrared Spectra, A Practical Approach*, in *Encyclopedia of Analytical Chemistry*, 2006, Wiley: Chichester, UK.
47. Zhang, C., et al., NaCl induced active hcp Co nanosheet for hydrogen production and formaldehyde abatement by formaldehyde steam reforming, *Chem. Eng. J.*, 2022, 433, 134600. https://doi.org/10.1016/j.cej.2022.134600
48. Zhao, X., Multi-scale multi-mechanism design of tough hydrogels: building dissipation into stretchy networks, *Soft Matter*, 2014, 10, 672-687. 10.1039/C3SM52272E
49. Kim, J., et al., Fracture, fatigue, and friction of polymers in which entanglements greatly outnumber cross-links, *Science*, 2021, 374, 6564, 212-216. 10.1126/science.abg6320
50. Brandenburg, J.E., et al., Feasibility and reliability of quantifying passive muscle stiffness in young children by using shear wave ultrasound elastography, *J. Ultrasound Med.*, 2015, 34, 4, 663-670. https://doi.org/10.7863/ultra.34.4.663
51. Leong, H.T., F. Hug, and S.N. Fu, Increased upper trapezius muscle stiffness in overhead athletes with rotator cuff tendinopathy, *PLoS One*, 2016, 11, 5, e0155187. 10.1371/journal.pone.0155187
52. Souron, R., et al., Sex differences in active tibialis anterior stiffness evaluated using supersonic shear imaging, *J. Biomech.*, 2016, 49, 14, 3534-3537. https://doi.org/10.1016/j.jbiomech.2016.08.008
53. Eby, S.F., et al., Shear wave elastography of passive skeletal muscle stiffness: Influences of sex and age throughout adulthood, *Clin. Biomech.*, 2015, 30, 1, 22-27. https://doi.org/10.1016/j.clinbiomech.2014.11.011
54. Wagner, S. and S. Bauer, Materials for stretchable electronics, *MRS Bull.*, 2012, 37, 3, 207-213. 10.1557/mrs.2012.37
55. Ding, H., et al., A semi-interpenetrating network ionic composite hydrogel with low modulus, fast self-recoverability and high conductivity as flexible sensor, *Carbohydr. Polym.*, 2020, 248, 116797. https://doi.org/10.1016/j.carbpol.2020.116797
56. Wang, A., et al., Hydrogen-bonded network enables semi-interpenetrating ionic conductive hydrogels with high stretchability and excellent fatigue resistance for capacitive/resistive bimodal sensors, *Chem. Eng. J.*, 2021, 411, 128506. https://doi.org/10.1016/j.cej.2021.128506
57. Liu, H., et al., Freezing-tolerant, highly sensitive strain and pressure sensors assembled from ionic conductive hydrogels with dynamic cross-links, *ACS Appl. Mater. Interfaces*, 2020, 12, 22, 25334-25344. 10.1021/acsami.0c06067
58. France-Lanord, A. and J.C. Grossman, Correlations from ion pairing and the Nernst-Einstein equation, *Phys. Rev. Lett. (8.6)*, 2019, 122, 13, 136001. 10.1103/PhysRevLett.122.136001
59. Lai, C.-W. and S.-S. Yu, 3D printable strain sensors from deep eutectic solvents and cellulose nanocrystals, *ACS Appl. Mater. Interfaces*, 2020, 12, 30, 34235-34244. 10.1021/acsami.0c11152
60. Song, J., et al., Mechanically and electronically robust transparent organohydrogel fibers, *Adv. Mater.*, 2020, 32, 8, 1906994. https://doi.org/10.1002/adma.201906994
61. Hao, S., et al., Tannic acid–silver dual catalysis induced rapid polymerization of conductive hydrogel sensors with excellent stretchability, self-adhesion, and strain-sensitivity properties, *ACS Appl. Mater. Interfaces*, 2020, 12, 50, 56509-56521. 10.1021/acsami.0c18250

Poly (vinyl alcohol)/Pullulan/NaCl Conductive Hydrogels for Wearable Strain Sensors

Xiaoyan Qing [a], Zhongda Liu [b], Alexandros Katsaounis [b], Nikolaos Bouropoulos [c,d], Irene Taurino [e,f], Pedro Fardim [a]*

[a] Chemical and Biochemical Reactor Engineering and Safety (CREaS), Department of Chemical Engineering, KU Leuven, Celestijnenlaan 200f, 3001 Leuven, Belgium. xiaoyan.qing@kuleuven.be

[b] Department of Chemical Engineering, University of Patras, Caratheodory 1 St, 26504 Patras, Greece. zhongda.liu@chemeng.upatras.gr; alex.katsaounis@chemeng.upatras.gr

[c] Department of Materials Science, University of Patras, 26504 Patras, Greece

[d] Foundation for Research and Technology Hellas, Institute of Chemical Engineering and High Temperature Chemical Processes, Stadiou Street, Platani, 26504 Patras, Greece. nbouro@upatras.gr

[e] Micro and Nano Systems (MNS), Department of Electrical Engineering, KU Leuven, 3001 Leuven, Belgium

[f] Semiconductor Physics, Department of Physics and Astronomy, KU Leuven, Celestijnenlaan 200d, 3001 Leuven, Belgium. irene.taurino@kuleuven.be

*Email: pedro.fardim@kuleuven.be

Supporting Tables

Table S1. Compositions of $PVA_x/Pullulan_y/NaCl_z$ hydrogels

Samples	Total polymer content (wt%)	x: PVA content in polymers (wt%)	y: Pullulan content in polymers (wt%)	z: NaCl concentration (M)
$PVA_{100}Pullulan_0$	12	100	0	-
$PVA_{98}Pullulan_2$	12	98	2	-
$PVA_{95}Pullulan_5$	12	95	5	-
$PVA_{90}Pullulan_{10}$	12	90	10	-
$PVA_{80}Pullulan_{20}$	12	80	20	-
$PVA_{70}Pullulan_{30}$	12	70	30	-
$PVA_{95}Pullulan_5NaCl_0$	12	95	5	0
$PVA_{95}Pullulan_5NaCl_{0.3}$	12	95	5	0.3
$PVA_{95}Pullulan_5NaCl_1$	12	95	5	1
$PVA_{95}Pullulan_5NaCl_2$	12	95	5	2
$PVA_{95}Pullulan_5NaCl_3$	12	95	5	3
$PVA_{95}Pullulan_5NaCl_4$	12	95	5	4
$PVA_{95}Pululan_5NaCl_5$	12	95	5	5
$PVA_{100}NaCl_{0.3}$	12	100	0	0.3
$PVA_{100}NaCl_1$	12	100	0	1
$PVA_{100}NaCl_2$	12	100	0	2
$PVA_{100}NaCl_3$	12	100	0	3
$PVA_{100}NaCl_4$	12	100	0	4
$PVA_{100}NaCl_5$	12	100	0	5

Note: "-" the hydrogels were not treated with NaCl solutions.

Table S2. Comparison of the mechanical properties and gauge factor with other similar PVA ionic (organo)hydrogels.

Hydrogel components	Tensile strength (MPa)	Ionic conductivity (S/m)	Gauge factor	Reference
$PVA_{95}/Pullulan_5/NaCl_{0.3}$	0.48	2.43	5.98	This work
$PVA_{95}/Pullulan_5/NaCl_1$	0.68	5.4	5.09	This work
$PVA_{95}/Pullulan_5/NaCl_2$	1.19	7.97	4.04	This work
$PVA_{95}/Pullulan_5/NaCl_3$	2.02	9.66	3.77	This work
$PVA_{95}/Pullulan_5/NaCl_4$	2.22	10.44	3.42	This work
$PVA_{95}/Pullulan_5/NaCl_5$	2.72	7.94	2.70	This work
PVA/PAM/Xanthan gum/$ZnCl_2$	1.14	3.098	4.4	[1]
PVA-TA/DMSO/NaCl	2.12	1.24	3.53	[2]
PVA/SA/Col/NaCl	0.39	3.8	3.36	[3]
Starch/PVA/EG/TA/$CaCl_2$	1.1	~1.37	2.96	[4]
TA@HAP NWs/PVA/$AlCl_3$/EG	0.36	1	2.84	[5]
PVA/CMCS/TA/NaCl/Gly	2.02	3.05	2.818	[6]
SF/PVA/Gly/LiCl	1.6	5.263	2.18	[7]
PVA/ι-CG/TA/$CaCl_2$	0.8	0.0585	2.15	[8]
PVA/NaCl	1.5	-	~2.1	[9]
PVA/LNP/EG/$AlCl_3$	1.241	1.35×10^{-2}	2.08	[10]
PVA/Urea/Na_3Cit	1.51	~0.6	1.94	[11]
PVA/Cellulose/TA/$Fe_2(SO_4)_3$	0.98	0.22	1.75	[12]
PVA/CNF/$ZnSO_4$	0.79	0.32	1.7	[13]
PVA/CMCS/Na_3Cit/$Al_2(SO_4)_3$	25.9	0.65	1.67	[14]
PVA/NaCl/Gly	1.4	~0.57	1.56	[15]
PVA/CNF/DMSO/NaCl	1.4	3.2	1.5	[16]

PVA/SS/Na_3Cit/Gly	6.92	0.67	1.49	[17]
PVA/Gly/NaCl	18.5	0.102	1.41	[18]
PVA/SS/Na_3Cit	3.93	0.83	1.4	[19]
PVA/EG/LiCl	-	0.67	1.2	[20]
PVA/Cellulose/$ZnCl_2$/$CaCl_2$	0.3	8.16	1.14	[21]
PVA/ANF/TA/DMSO/$CaCl_2$	6.25	3.09	1.02	[22]
PVA/NaCl	8.03	7.14	0.989	[23]
PAA-PVA/PAM/$ZnSO_4$	9.45	0.189	0.68	[24]
PVA-Gelatin/$FeCl_3$	2.466	-	0.55	[25]
PVA/PAM/GA-$ZnCl_2$	0.25	~0.014	0.209	[26]
PVA/PA-$FeCl_3$	1.22	4.91	-	[27]

Note: "-" the value was not mentioned.

Abbreviations

PVA, Poly(vinyl alcohol); PAM, Polyacrylamide; TA, Tannic acid; DMSO, Dimethyl sulfoxide; SA, Sodium alginate; Col, Collagen; EG, Ethylene glycol; HAP NWs, Hydroxyapatite nanowires; CMCS, Carboxymethyl chitosan; Gly, Glycerol; SF, Silk fibroin; ι-CG, ι-carrageenan; LNP, Nanolignin; CNF, Cellulose nanofibrils; SS, Silk sericin; ANF, Ramid nanofibers; PAA, Poly(acrylic acid); GA, Gallic acid; PA, Phytic acid.

Supporting Figures

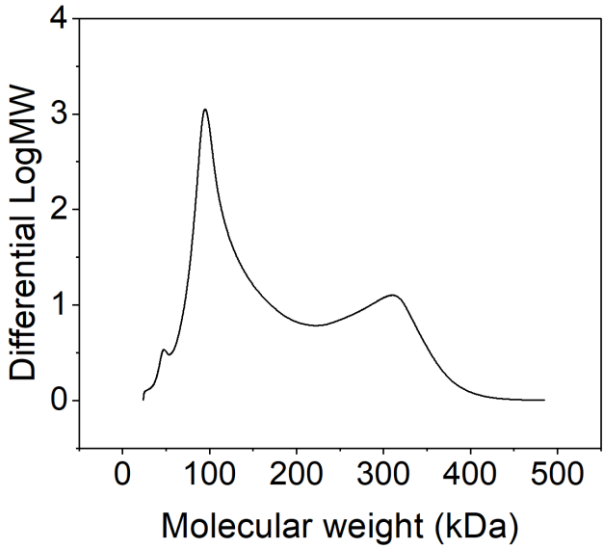

Figure S1. Molecular distribution of pullulan. The molecular weights of pullulan were determined by GPC. The results showed that the number-average (Mn), weight-average (Mw), and Z-average (Mz) molecular weight of pullulan were 97.51 kDa, 136.72 kDa and 180.67 kDa, respectively.

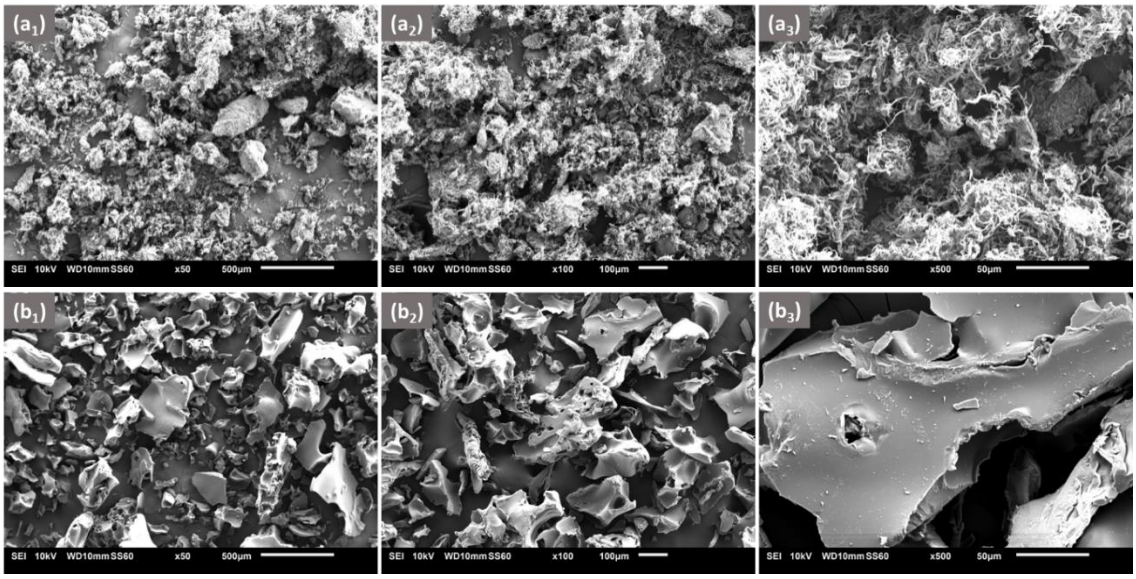

Figure S2. SEM of (a_1) ˣ50, (a_2) ˣ100, and (a_3) ˣ500 of PVA, (b_1) ˣ50, (b_2) ˣ100, and (b_3) ˣ500 of pullulan.

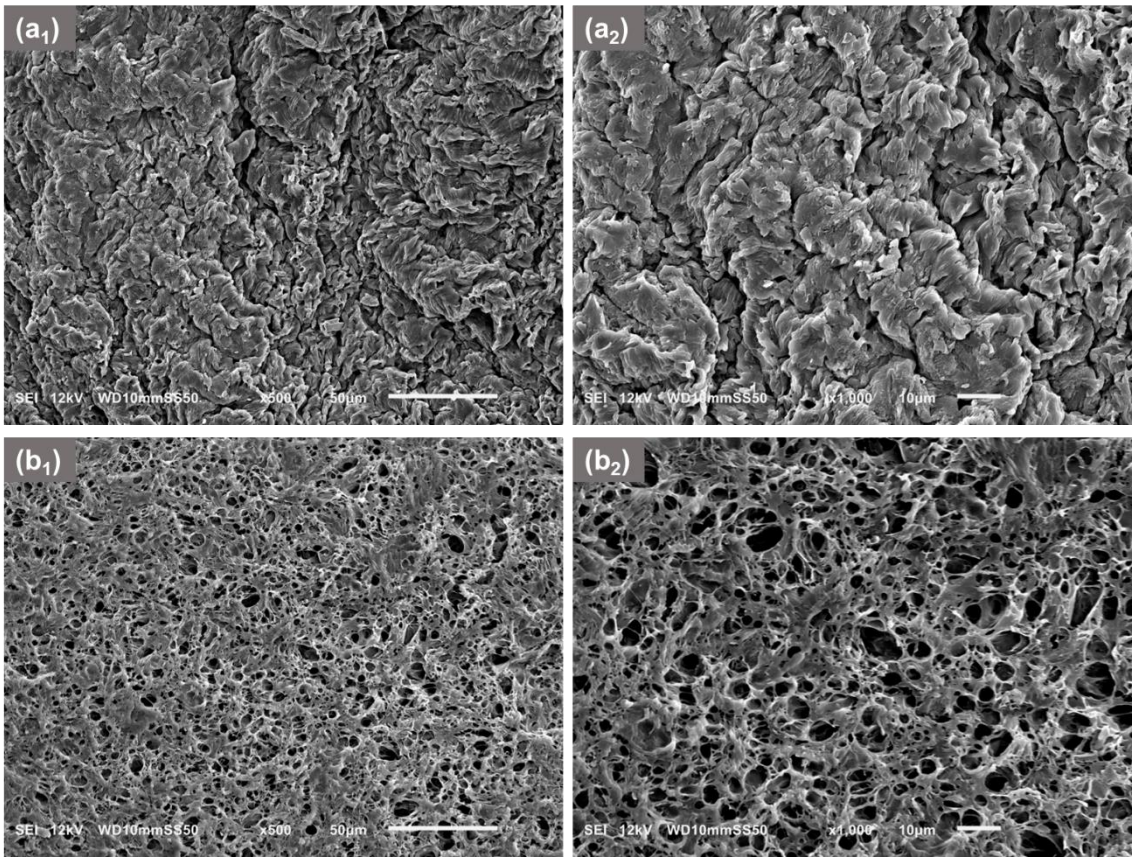

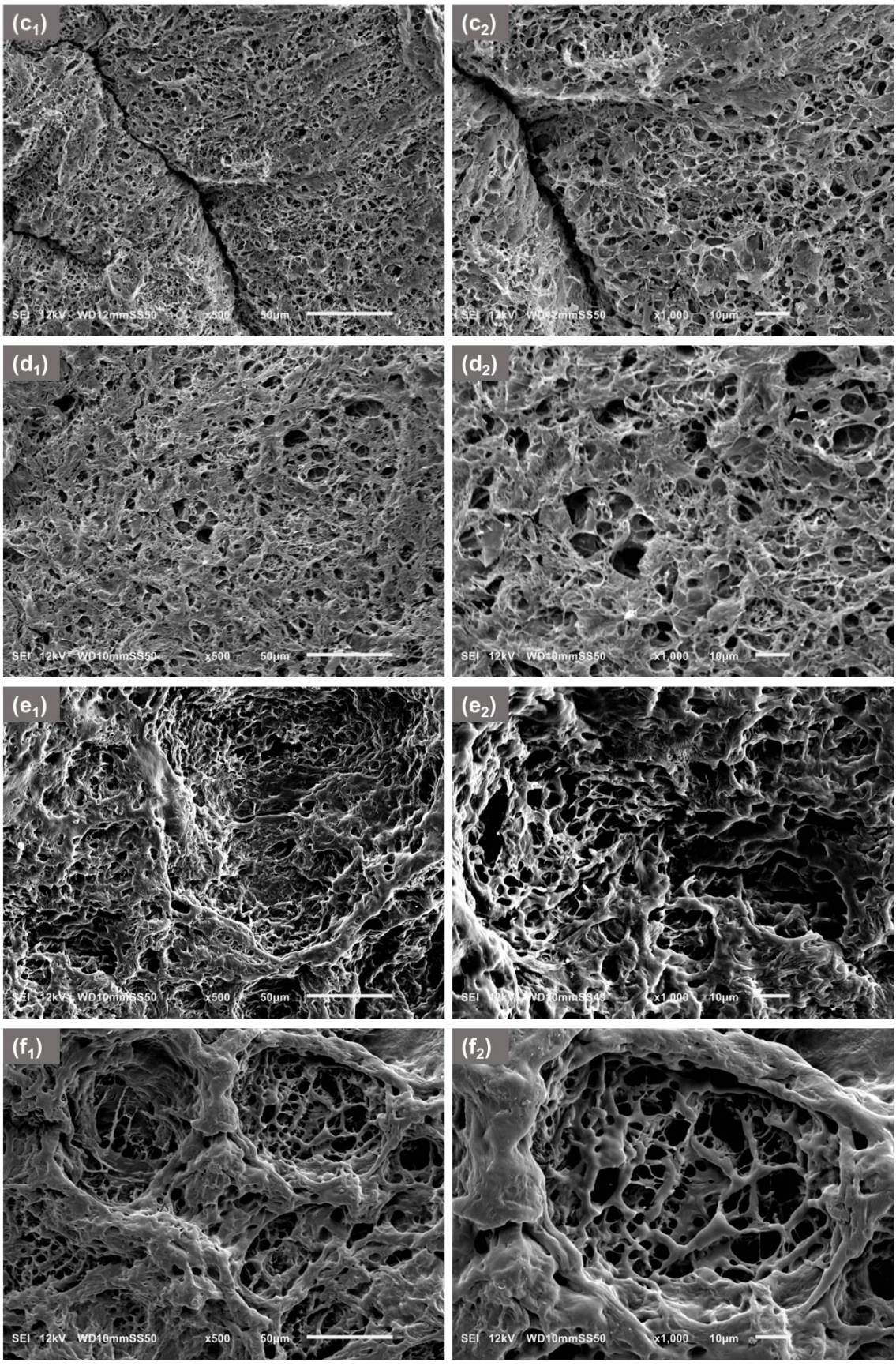

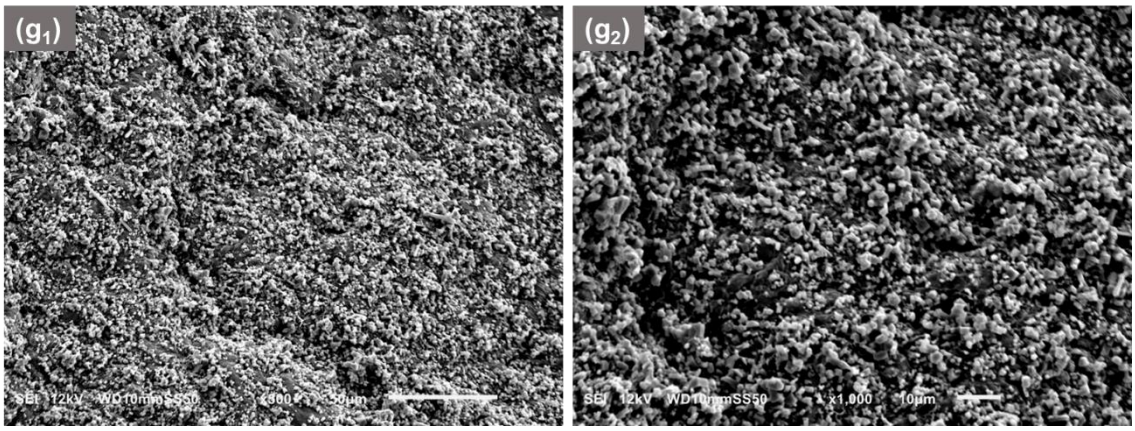

Figure S3. SEM of hydrogels. (a_1) ×500, and (a_2) ×1000 of pure PVA hydrogel, (b_1) ×500, and (b_2) ×1000 of PVA_{98}/$Pullulan_2$ hydrogel, (c_1) ×500, and (c_2) ×1000 of PVA_{95}/$Pullulan_5$ hydrogel, (d_1) ×500, and (d_2) ×1000 of PVA_{90}/$Pullulan_{10}$ hydrogel, (e_1) ×500, and (e_2) ×1000 of PVA_{80}/$Pullulan_{20}$ hydrogel, (f_1) ×500, and (f_2) ×1000 of PVA_{70}/$Pullulan_{30}$ hydrogel, (g_1) ×500, and (g_2) ×1000 of PVA_{95}/$Pullulan_5$/$NaCl_1$ hydrogel.

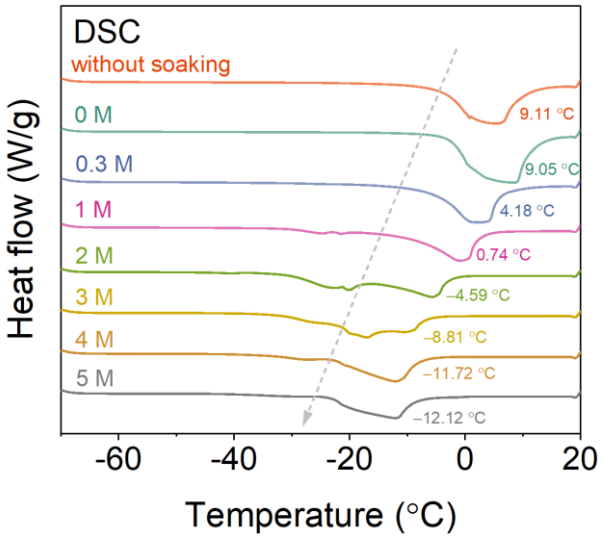

Figure S4. DSC curves of the PVA_{95}/$Pullulan_5$/$NaCl_z$ hydrogels.

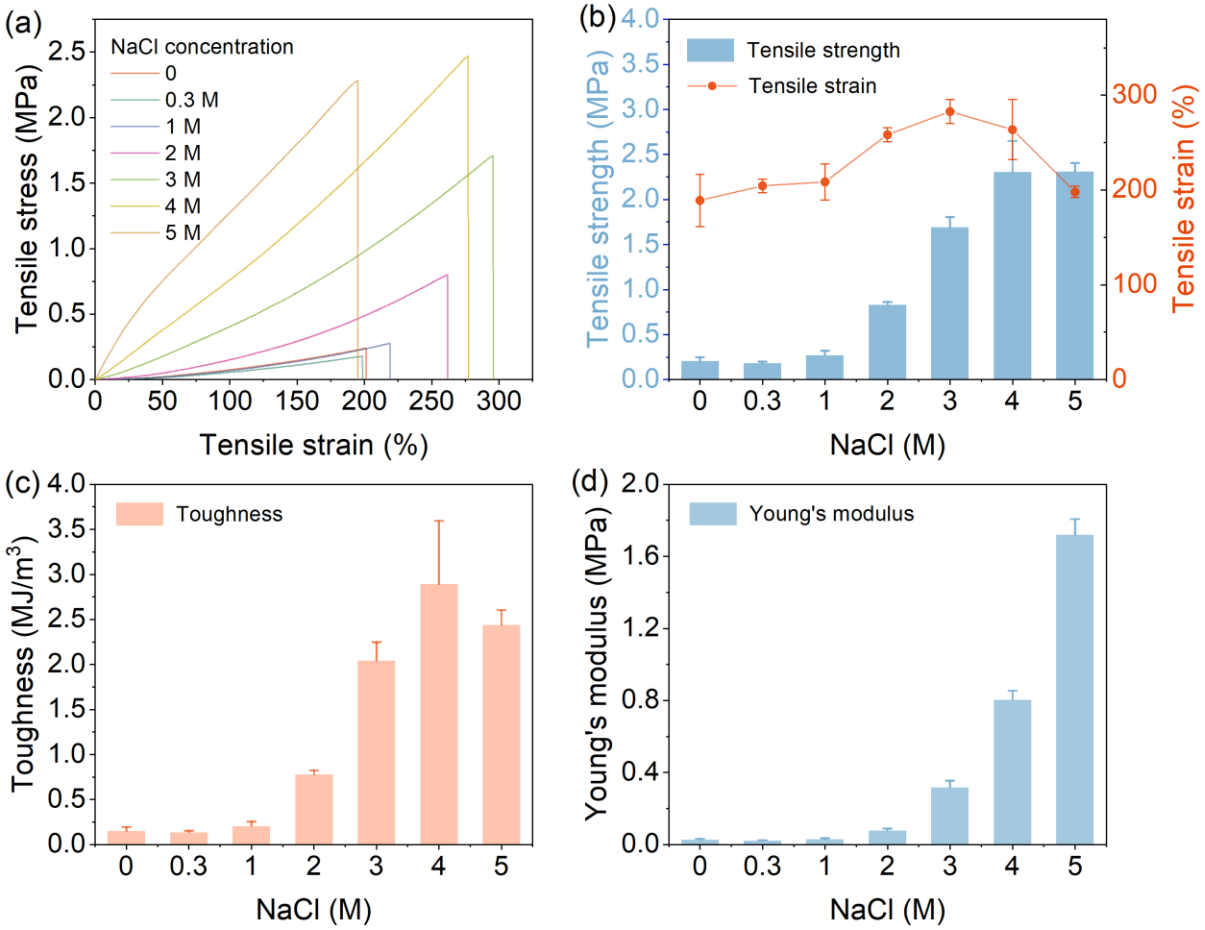

Figure S5. Mechanical properties of PVA/NaCl hydrogels, including (a) tensile stress-tensile strain, (b) tensile strength and tensile strain, (c) toughness, and (d) Young's modulus.

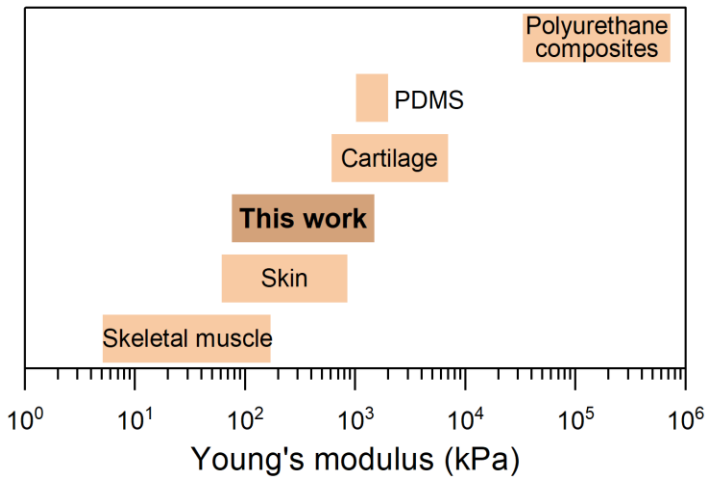

Figure S6. Young's modulus comparison of PVA/Pullulan/NaCl hydrogels with that of human tissues and common traditional materials in stretchable electronics.

Reference

1. Zhou, Y., et al., Dual-network polyvinyl alcohol/polyacrylamide/xanthan gum ionic conductive hydrogels for flexible electronic devices, *Int. J. Biol. Macromol.*, 2023. 233, 123573.
2. Zou, Y., et al., Highly mechanical properties, anti-freezing, and ionic conductive organohydrogel for wearable sensors, *React. Funct. Polym.*, 2022. 175, 105267.
3. Xia, S., et al., Recyclable hydrogel for human-machine interface of multi-mode human vital signal acquisition, *Sci. China Mater.*, 2023. 66, 7, 2843–2851.
4. He, L., et al., A high-strength, environmentally stable, self-healable, and recyclable starch/PVA organohydrogel for strain sensor, *Eur. Polym. J.*, 2022. 181, 111650.
5. Wen, J., et al., Multifunctional ionic skin with sensing, UV-filtering, water-retaining, and anti-freezing capabilities, *Adv. Funct. Mater.*, 2021. 31, 21, 2011176.
6. Zhang, L., et al., Preparation of tough and ionic conductive PVA/carboxymethyl chitosan bio-based organohydrogels with long-term stability for strain sensor, *Cellulose*, 2022. 29, 9323–9339.
7. Tao, X.Y., et al., Recyclable, anti-freezing and anti-drying silk fibroin-based hydrogels for ultrasensitive strain sensors and all-hydrogel-state super-capacitors, *Mater. Today Chem.*, 2023. 32, 101624.
8. Zeng, L., et al., Tough, recyclable and biocompatible carrageenan-modified polyvinyl alcohol ionic hydrogel with physical cross-linked for multimodal sensing, *Int. J. Biol. Macromol.*, 2023. 253, 126954.
9. Wang, Q., et al., Muscle-inspired anisotropic hydrogel strain sensors, *ACS Appl. Mater. Interfaces*, 2022. 14, 1, 1921–1928.
10. Wang, Y., et al., Nanolignin filled conductive hydrogel with improved mechanical, anti-freezing, UV-shielding and transparent properties for strain sensing application, *Int. J. Biol. Macromol.*, 2022. 20,: 442–451.
11. Ye, W., et al., High strength, anti-freezing, and conductive poly(vinyl alcohol)/urea ionic hydrogels as soft sensor, *Polym. Eng. Sci*., 2022. 62, 12, 3985–3993.
12. Hu, J., et al., Multi-physics coupling reinforced polyvinyl alcohol/cellulose nanofibrils based multifunctional hydrogel sensor for human motion monitoring, *Int. J. Biol. Macromol.*, 2023. 235, 123841.
13. Hu, J., et al., One-pot freezing-thawing preparation of cellulose nanofibrils reinforced polyvinyl alcohol based ionic hydrogel strain sensor for human motion monitoring, *Carbohydr. Polym.*, 2022, 275, 118697.
14. Zhang, L., et al., Super strong and tough anisotropic hydrogels through synergy of directional freeze-casting, metal complexation and salting out, *Chem. Eng. J*., 2023, 463, 142414.
15. Zha, X.-J., et al., Nanofibrillar poly(vinyl alcohol) ionic organohydrogels for smart contact lens and human-interactive sensing, *ACS Appl. Mater. Interfaces*, 2020, 12, 20, 23514–23522.
16. Ye, Y., et al., Cellulose nanofibrils enhanced, strong, stretchable, freezing-tolerant ionic conductive organohydrogel for multi-functional sensors, *Adv. Funct. Mater.*, 2020. 30, 35, 2003430.
17. Fu, H., et al., Super tough, stretchable and transparent ionic conductive hydrogel for flexible sensor with excellent temperature tolerance, *React. Funct. Polym.*, 2023, 186, 105572.
18. Xiang, C., et al., A self-reinforced tough and multifunctional polyvinyl alcohol fabric composite hydrogel, *Compos Sci Technol*., 2023, 243, 110212.
19. Wang, F., et al., Highly strong, tough, and stretchable conductive hydrogels based on silk sericin-mediated multiple physical interactions for flexible sensors, *ACS Appl. Mater. Interfaces*, 2022, 4, 1, 618–626.
20. Yang, J., et al., Facile preparation and characterization of tough poly(vinyl alcohol) organohydrogels with low friction and self-cleaning properties, *J. Ind. Eng. Chem*., 2022, 116, 207–216.
21. Shu, L., et al., Facile fabrication of strong and conductive cellulose hydrogels with wide temperature tolerance for flexible sensors, *Int. J. Biol. Macromol.*, 2023, 240, 124438.
22. Wu, W., et al., Synergistic strengthening of PVA ionic conductive hydrogels using aramid nanofibers and tannic acid for mechanically robust, antifreezing, water-retaining and antibacterial flexible sensors, *J. Colloid Interface Sci.*, 2023, 654, 1260–1271.
23. Di, X., et al., High-performance ionic conductive poly(vinyl alcohol) hydrogels for flexible strain sensors based on a universal soaking strategy, *Mater. Chem. Front.*, 2021, 5, 315–323.
24. Zheng, B., et al., Fishing net-inspired mutiscale ionic organohydrogels with outstanding mechanical robustness for flexible electronic devices, *Adv. Funct. Mater.*, 2023. 33, 28, 2213501.

25. Sun, S., Y. Xu, and X. Maimaitiyiming, Tough polyvinyl alcohol-gelatin biological macromolecules ionic hydrogel temperature, humidity, stress and strain, sensors, *Int. J. Biol. Macromol.*, 2023, 249, 125978.
26. Yuan, H., et al., Plant-derived adhesive hydrogel with high stretchability and conductivity for wearable electronics, *Sens. Actuators B Chem.*, 2023, 379, 133195.
27. Liu, Z., et al., One-pot preparation of tough, anti-swelling, antibacterial and conductive multiple-crosslinked hydrogels assisted by phytic acid and ferric trichloride, *J. Appl. Polym. Sci.*, 2023. 140, 32, e54243.